RSC Advances

PAPER

View Article Online
View Journal | View Issue

Cite this: *RSC Adv.*, 2024, **14**, 23952

A novel mucoadhesive paliperidone-nanoemulsion developed using the ultrasonication method in the treatment of schizophrenia

Niyaz Ahmad, *[ab] Khalid Ansari,[c] Mariam K. Alamoudi,[d] Anzarul Haque,[e] Zabih Ullah,[f] Mohammed Saifuddin Khalid[g] and Sarfaraz Ahmad[h]

Aim: To develop paliperidone mucoadhesive-nanoemulsion (PLP-NE) to enhance brain bioavailability. To evaluate comparative effects of PLP-NE and CS-PLP-NE in the treatment of schizophrenia, followed by a toxicity study of opt-NE. *Material and methods*: Oil: oleic acid, surfactant: Tween-80, and co-surfactant: Labrasol were chosen based on the solubility and maximum nanoemulsion area. The ultrasonication technique was applied with the aqueous micro titration method for the development of PLP-NE. The optimization of the method for the excellent PLP-NE was performed using a central composite design based on a five-factor and four-level. Oil (% v/v), S_{mix} (v/v%), ultrasonication intensity in percentage, ultrasonication time in minutes, and temperature (°C) were optimized and used to the independent variables. *Results*: The parameters *i.e.*, oil (5%), S_{mix} (10%), ultrasonication time (5.0 min), ultrasonication intensity (25%), and temperature (38 °C) were optimized and used as independent and dependent variables for the development of novel PLP-NE. Based on experimental data, the dependent variables, *i.e.*, globule size (53.90 ± 4.01 nm), % transmittance (92.56% ± 1.06%), PDI (0.218 ± 0.007), and zeta potential (−11.60 ± 0.031 mV), were determined. The smooth near about spherical shaped of PLP-NE globules with, refractive index *i.e.*, 1.62 ± 0.021, viscosity: 39 ± 6 cp with the pH: 7.40 ± 0.089, and content of drug (97.98 ± 0.39%) for optimized-PLP-NE. The optimized PLP-NE with oleic acid, Tween-80, and Labrasol was used to improve brain bioavailability with good permeation *via* the intranasal route. CS-PLP-NE yielded good mucoadhesive property results compared to paliperidone-nanoemulsion, and PLP-S containing a 0.751 minutes retention time with their deuterated-IS (0.806 min) and *m*/*z* of 427.2/207.2 with IS (*m*/*z*: 431.2/211.2) for PLP and PLP-IS. A calibration curve was plotted with a linear range of 1–2000 ng mL^{-1} with inter- and intraday accuracy (97.03–99.31%) and precision (1.69–50.05%). The results of $AUC_{(0-24)}$ and C_{max} for PLP were found to be highly significant ($p < 0.001$) as an improvement of brain bioavailability in rats *via* intranasal delivery of CS-PLP-NE. Furthermore, the locomotion test, social interaction, and forced swimming test (forced swimming, climbing, and immobility) of a mucoadhesive CS-PLP-NE (intranasally) provided highly significant results with the improvement of behavioral analysis when compared to the PLP-NE and PLP-S studies. *Conclusion*: CS-PLP-NE (i.n.) showed highly significant results, *i.e.*, $p < 0.001$ for the improvement of bioavailability of the brain in the treatment of schizophrenia. Optimized-mucoadhesive-CS-based-PLP-NE is safe and shows no toxicity.

Received 25th June 2024
Accepted 11th July 2024

DOI: 10.1039/d4ra04624b

rsc.li/rsc-advances

Introduction

Schizophrenia is the most important mental disorder affecting more than twenty-one million people worldwide.[1] It has been the most dominant antipsychotic disorder for its treatment over the last 70 years. The psychotic symptoms were reduced by first-generation antipsychotics (FGAs) and second-generation antipsychotics (SGAs). Atypical antipsychotics have been given

[a]*Department of Pharmaceutics, College of Dentistry and Pharmacy, Buraydah Colleges, Buraydah, Alqassim, Saudi Arabia. E-mail: niyazpharma@gmail.com; Niyaz.Husain@bpc.edu.sa; Tel: +966 531203626*

[b]*Department of Pharmaceutical Sciences, Green Lab, Riyadh, Saudi Arabia*

[c]*Liwa College, Faculty of Medical and Health Sciences, Abu Dhabi, United Arab Emirates*

[d]*Department of Pharmacology, College of Pharmacy, Prince Sattam Bin Abdulaziz University, Al-Kharj 11942, Saudi Arabia*

[e]*Central Laboratories Unit, Qatar University, Doha 2713, Qatar*

[f]*Department of Pharmaceutical Sciences, College of Dentistry and Pharmacy, Buraydah Colleges, Alqassim, Saudi Arabia*

[g]*Department of Pharmacology, College of Clinical Pharmacy, Imam Abdulrahman Bin Faisal University, Dammam, Saudi Arabia*

[h]*Department of Clinical Pharmacy, College of Pharmacy, Jazan University, Jazan 114, Saudi Arabia*

preference for the incidence of EPS (extrapyramidal symptoms) based on their effective treatment doses, thereby improving the quality of life of patients.[2,3] The drug should be soluble in lipids to cross the BBB (blood–brain barrier). However, it was generally observed that most antipsychotic drugs are water soluble, which is the opposite of reaching the targeted site of treatment, *i.e.*, in the brain with optimum quantity. Finally, it showed a very low bioavailability of antipsychotic drugs and produced sub-therapeutic effects. Increasing their dose results in adverse effects.[4] It is not a good solution to enhance the dose of the drugs for effective treatment because there is a narrow therapeutic window. Despite improvements in the field of medicine/medical treatments, adverse effects and extrapyramidal symptoms continue to be prominent problems that prevent treatment to the patient's compliance and faithfulness.[5]

Paliperidone (PLP) was categorised as a second-generation atypical antipsychotic drug in the treatment of schizophrenia. PLP antagonized the D2-based dopamine type 2 and 5-HT2A, *i.e.*, central serotonin type 2 receptors.[6] In addition, PLP has been reported to have antioxidant and anti-inflammatory properties that are helpful in the treatment of schizophrenia. Oxidative stress might be recognised for the enhancement of dopamine activity, which produces ROS (reactive oxygen species). It was generally observed in schizophrenic patients for the production of free radicals due to neuronal damage. In this case, the drugs have an antioxidant property that can be helpful in their treatment.[7] PLP showed antioxidant properties due to a reduction in the production of ROS, followed by a decrease in lipid peroxidation. It was previously reported in rats. PLP reduced the quantity of dopamine by reducing the levels of redox enzymes (*e.g.*, catalase, adenosine deaminase, and xanthine oxidase). This helped in the treatment of psychotic patients by showing hallucinations and delusions.[8] It has also been reported in different studies that PLP plays a potential role as an antioxidant and antiinflammatory.[9]

The researchers were also facing difficulties in the treatment of brain disorders due to the covering of the brain, *i.e.*, BBB, from various years. It is very challenging to target brain-related disorders or diseases. The blood–brain barrier (BBB) plays a crucial role in safeguarding the brain against external substances while regulating the internal balance of brain tissues. Consequently, delivering drugs directly to brain tissue *via* the bloodstream poses a significant challenge in the treatment of brain disorders.[10] The BBB's primary function is to shield the brain from foreign substances. Additionally, the BBB plays a role in maintaining the internal equilibrium of brain tissues. Hence, it is very difficult to transport the drug directly into the brain from blood flow peripherally in the treatment of brain disorders.[10] Nanotechnology is currently the best option for targeting the brain to improve its bioavailability and treatment by developing a novel nanoformulation. In the present research, paliperidone is converted first into nanoemulsion to improve the bioavailability of PLP in the brain.[11,12] Currently, most scientists are working on the intranasal drug delivery system as a tool to target the drug into the brain to avoid first-pass metabolism. This showed many advantages, such as drugs being delivered easily *via* a non-invasive route, followed by avoiding the peripherally produced adverse/side effects of the drugs.[13,14] There are some other advantages for the drugs targeted and easily delivered by the i.n. route: they produce results effectively, are painless, are very safe, and require a very small amount of drug delivered to the brain *via* the olfactory lobe. Based on facts and literature surveys, it has been confirmed that the best delivery route for brain targeting is the intranasal route.[14]

Therefore, the development of a novel nanoemulsion is a requirement of this proposed research to target the brain. Paliperidone was incorporated into the nanoemulsion "new wine in an old bottle". There is a new formulation technique for the development of nanocarriers. The nanoemulsion still dominates the foothold because of the ease of manufacturing and scale-up possibility. The drug is encapsulated inside the NE to improve its efficiency by improving its solubility and bioavailability.[15] It was very confusing before between the nanoemulsion and microemulsion, which means that there is no change, meaning that both have the same formulations that were used interchangeably. The use of surfactant in the preparations of microemulsion required a high quantity near about more than 20% compared to nanoemulsions. Therefore, microemulsions are thermodynamically stable.[16] The nanoemulsion showed a smaller diameter of globule sizes compared to the microemulsion.[17] There are some limitations to the use of a high quantity of surfactants internally. However, the development of nanoemulsions requires a small quantity of surfactants that can be used internally, but they should be kinetically stable. It was previously reported that nanoemulsion preparation is not spontaneous ($\Delta G > 0$). Therefore, it requires external energy at the time of manufacturing.[18] Therefore, this research is based on the preparation of a paliperidone nanoemulsion (PLP-NE) using ultrasonication techniques as an external energy source to fabricate the nanoemulsion with the help of the chemical engineering of a combination of oil and surfactants. The CCD methodology was employed to optimize the parameters of the PLP-NE. These parameters, including the oil concentration (expressed as % v/v), S_{mix} concentration (also % v/v), ultrasonication intensity (in percentage), ultrasonication time (in minutes), and temperature (in °C), were systematically adjusted to develop the most effective PLP nanoemulsion. The optimization aimed to enhance various dependent variables such as globule size, % transmittance, Polydispersity Index (PDI), and zeta potential. Finally, a mucoadhesive nanoemulsion of paliperidone was prepared from the conversion of opt-PLP-NE that increased the nasal staying time, *i.e.*, a very important criterion for targeting the brain or brain tissues.[12]

There is no literature available to date for any bioanalytical method of brain tissue of PLP to conduct the brain pharmacokinetic study.[19–23] Therefore, this study developed and successfully validated a novel highly sensitive up to picogram level LC-MS-based bioanalytical method to perform a comparative pharmacokinetic study of PLP-NE with mucoadhesive CS-PLP-NE and PLP-simple suspension from different routes of administration in the brain and plasma. In this research, we also compared the behavioural study of PLP-NE with mucoadhesive CS-PLP-NE as well as PLP-simple suspension from

different routes of administration. Finally, we conducted a toxicity study and optimized a novel mucoadhesive CS-PLP-NE.

Materials and methods

Materials

Sun Pharmaceutical Industries Ltd (India) gave us paliperidone. An ultra-pure water purification system (Avidity Science, UK) was used to filter the water to produce the ultra-pure water. We purchased many ingredients from Sigma (Tween 80, Oleic acid, Labrasol, *etc.*). All the chemicals used in this research were highly pure (99.9%) and were obtained from Sigma.

Screening of ingredients for the development of PLP-NE

The excipients were selected based on the solubility of PLP with co-surfactant, oil, and surfactant and also prepared the stable NE. We selected the oil phase: oleic acid, surfactant: Tween 80, and co-surfactant: Labrasol based on the solubility of the drug, as mentioned in Table 1, with their zeta potential value for vehicles in various combinations. However, all of them exhibited a high zeta potential value when compared to these three combinations. ZP showed a negative value that could be due to fatty acid esters containing a negative charge in the oleic acid. Both Tween 80 (HLB: 15.0) and Labrasol (HLB: 8–12) are nonionic surfactants.[24,25]

Pseudoternary phase diagram (PTPD) study for the optimization of nanoemulsion

We employed the aqueous microtitration technique to formulate a novel nanoemulsion devoid of any active drug that served as a placebo nanoemulsion. This involved using a 5.0 mL screw-capped glass vial into which we introduced the chosen oil, surfactant, and co-surfactant (S_{mix}), ensuring thorough mixing. For the optimization of nanoemulsion, the titration was performed with ultra-pure water.[28] The surfactant quantity was optimized based on the use of different types of S_{mix} ratios, including 1 : 1, 4 : 1, 2 : 1, 1 : 3, 5 : 1, 1 : 2, and 3 : 1. In the higher and wider nanoemulsion occupied area, there were significant variations in the different quantities of oil and S_{mix} ratios, such as 1 : 7, 1 : 9, 1 : 3.5, 1 : 8, 1 : 6, 1 : 3, 1 : 5, 2 : 8, 4 : 6, 1 : 2, 6 : 4, 3 : 7, 5 : 5, 9 : 1, 8 : 2, and 7 : 3. Considering the variables, each S_{mix} ratio resulted in fifty-one different preparations. In total, 97 formulations were formulated based on the 6 different types of ratios of S_{mix}. In accordance with the PTPD region, all formulations were prepared and optimized based on clear visual observation during microtitration, resulting in the preparation of a placebo nanoemulsion.

Paliperidone-nanoemulsion (PLP-NE) development and optimization

The PLP-NE was prepared using a high-energy ultrasonication technique. Initially, PLP was dissolved in the oil phase, along with S_{mix}, in a glass vial. This mixture was then micro-titrated with ultra-pure to obtain the coarse nanoemulsion. To produce a novel nanoemulsion, a 20 kHz ultrasonic processor from Fisher Scientific Technology, USA, was employed. This ultrasonic processor operated at 500 Watts of power and was equipped with a titanium horn with a 1 mm diameter for the preparation of the nanoemulsion. In summary, the preparation of PLP-NE involved the use of optimized parameters, including an ultrasonication intensity of 25.0%, an ultrasonication time of 5.0 minutes, and a temperature of 38.0 °C. These conditions were applied to transform the coarse PLP emulsion into PLP-NE, as described by Singh *et al.*[27] "Cavitation" is a phenomenon driven by a force that can generate heat.[30] Consequently, the temperature (°C) chosen and time (minutes) become crucial parameters for the formulation and optimization of paliperidone nanoemulsion, as highlighted in studies by Ghosh *et al.*[29] and Li *et al.*[26] PLP-NE exhibits a significantly low size of globules, typically <100 nm, resulting in enhanced Brownian motion. This characteristic contributes to the kinetic stability of PLP-NE, which is a crucial requirement for long-term storage, as emphasized in the work by McClements *et al.*[17]

Optimization of paliperidone-loaded nanoemulsion using CCD design

Design Expert is a popular software package used for the design of experiments and statistical analyses, including response surface methodology involving several factors and levels to optimize PLP-NE. Central Composite Design (CCD) and Box–

Table 1 Paliperidone solubility in different oils and surfactants

S. no.	Name of the vehicle	Solubility (mg g^{-1} or mg mL^{-1})	S. no.	Name of the vehicle	Solubility (mg g^{-1} or mg mL^{-1})
1	Labrasol	29.3 ± 1.37	12	Transcutol	51.9 ± 3.8
2	Linoleic acid	13.8 ± 0.4	13	Tween 80	11.41 ± 2.06
3	Oleic acid	54.69 ± 5.67	14	Cremophor RH	3.69 ± 0.86
4	Glycerol	2.81 ± 0.4	15	Medium chain triglyceride	1.49 ± 0.65
5	PEG 400	8.63 ± 0.5	16	Tween 20	10.39 ± 1.09
6	PEG 300	11.2 ± 0.98	17	Tween 60	4.5 ± 1.06
7	PEG 200	2.69 ± 0.69	18	Span 20	2.85 ± 0.95
8	Captex 200P	1.83 ± 3.81	19	Gelucire-44/14	3.95 ± 1.16
9	Lauroglycol FCC	5.69 ± 1.62	20	Labrafil 1944 CS	8.79 ± 2.23
10	Capryol	14.85 ± 1.03	21	Plurol oleique	16.87 ± 3.13
11	Capmul MCM	12.13 ± 1.86	22	Captex 355	5.91 ± 1.09

Behnken Design (BBD) are both popular experimental designs used in response surface methodology (RSM) for optimization in pharmaceutical research, among other fields. In terms of improved response prediction, CCD was selected as the superior option when compared to BBD in a study conducted by Loong *et al.*[30] BBD has certain limitations concerning recommendations, specifically its use of only low, medium, and high values to formulate independent variables. However, CCD provides an advantage by incorporating two additional values ($+\alpha$ and $-\alpha$), making it a favorable design that meets rotatability requirements in addition to the values included in BBD (Table 2).

In this research, we utilized the CCD approach to optimize the nanoemulsion. Within the framework of CCD, we optimized several dependent variables, including globule size (measured in nm), Zeta Potential (ZP), % transmittance, and Polydispersity Index (PDI). Concurrently, we considered independent variables (IV), such as oil percentage (%), S_{mix} percentage (%), ultrasonication time (measured in minutes), ultrasonication intensity (expressed as a percentage), and temperature (measured in degrees Celsius). Furthermore, selected 5-independent variables (IVs), specifically the percentages of oil and S_{mix}, were designated as composition variables, while ultrasonication intensity, ultrasonication time, and temperature were considered process variables. The selection of high and low levels for the composition of oil and surfactant was based on the PTPD, while the software automatically assigned the $-\alpha$ and $+\alpha$ levels. In accordance with the CCD recommendation for inputting IV values, 50 randomized formulations were conducted. Out of these, 32 were chosen, comprising factorial points, axial points (10), and center points (8), as shown in Table 3. Consequently, all the stipulated constraints align with the necessary criteria to optimize the most favorable formulation. A quadratic polynomial equation was produced by the CCD software for a 5-factor-4-level design as follows:

$$Y = b_0 + b_5X_5 + b_6X_6 + b_7X_7 + b_{56}X_5X_6 + b_{57}X_5X_7 + b_{57}X_5X_7 + b_{55}X_5^2 + b_{66}X_6^2 + b_{77}X_7^2.$$

Table 2 Variables in "Design Expert" software for the preparation and optimization of paliperidone nanoemulsions (PLP-NE)

Factors	Levels		
Independent variables	Low (−1)	Medium (0)	High (+1)
X_1 = oil (% v/v)	2.5	5.0	7.5
X_2 = S_{mix} (% v/v)	10	15	20
X_3 = ultrasonication time (min)	3	6	9
X_4 = ultrasonication intensity (%)	20	40	60
X_5 = temperature (°C)	30	40	50
Independent variables	**Constraints**		**Importance**
X_1 = oil (% v/v)	In range		− − − − − −
X_2 = S_{mix} (% v/v)	Minimize		+ + + +
X_3 = ultrasonication time (min)	In range		− − − − − − −
X_4 = ultrasonication intensity (%)	Minimize		+ + + + + +
X_5 = temperature (°C)	In range		− − − − − − −
Dependent variables			
Y_1 = globule size (nm)	Minimize		+ + + + +
Y_2 = transmittance (%)	Maximize		+ + + + + + +
Y_3 = polydispersity index (PDI)	Maximize		+ + + +
Y_4 = zeta potential (mV)	Minimize		+ + + +

Evaluating the parameters for the characterization of nanoemulsion

The measurements of mean droplet size (DS) and PDI were conducted at 25 °C using a Malvern Zetasizer based on dynamic light scattering principles. Disposable capillary cuvettes with electrodes were employed to observe the size of the particles. As previously indicated by Ahmad *et al.*,[24] a 100-fold dilution of the samples with double-distilled water was performed prior to measurement to mitigate the potential for multiple scattering effects. The mean droplet size and PDI were then calculated based on an average of thirteen measurements taken at an angle of 173°.

Analysis of the particle surface charge (ZP)

The ZP was examined using electrophoretic mobility measurements with the Malvern Zetasizer set to maintain refractive index and viscosity values at 1.62 ± 0.021 and 0.91 cp, respectively, to replicate the properties of pure water. Following the droplet size measurements, the ZP was assessed with three consecutive readings recorded for each sample. The mean value and standard deviation were then calculated, as described by Ahmad *et al.*[24]

SEM technique

Surface texture analysis for the optimized PLP-NE was conducted using scanning electron microscopy with a Zeiss EVO40 instrument (Carl Zeiss, Cambridge, UK). In summary, sample spreading was accomplished using double-sided conductive tape, followed by gold coating of the surface using an SCD020 Blazers sputter coater unit (BAL-TEC GmbH, Witten, Germany) under high vacuum conditions. The sputter unit was preconditioned with argon gas for 100 seconds at 50 mA.[24]

Transmittance (%) study

To assess the globule size and formulation stability, we conducted spectrophotometric measurements of percent transmittance at 650 nm using a Shimadzu UV-1601 spectrophotometer in Kyoto, Japan. We utilized distilled water as the solvent and maintained the original concentration for all formulations following the procedure outlined by Ahmad *et al.*[24]

The method of preparation of mucoadhesive- paliperidone-nanoemulsion

The method described above was employed for the formulation of opt-PLP-NE. We incorporated a 1% w/v chitosan (CS) solution into the PLP-NE drop by drop while continuously vortexing for 10.0 minutes. This process resulted in the formation of a clear and transparent mucoadhesive PLP-NE with chitosan (CS-PLP-NE), as detailed by Ahmad *et al.*[12]

Table 3 Nanoemulsions trials performed using "Design Expert" software at independent variables and their responses

Formulation code	Independent variables: Coded factors					Dependent variables: Observed responses				Predicted responses			
	X_1	X_2	X_3	X_4	X_5	Y_1	Y_2	Y_3	Y_4	Y_1	Y_2	Y_3	Y_4
NanE1	2.5	10	3	10	30	111.92 ± 11.64	88.27 ± 3.16	0.413 ± 0.003	−17.14 ± 2.33	111.09	88.39	0.4099	−17.14
NanE2	7.5	10	3	10	30	85.38 ± 7.26	87.93 ± 2.48	0.444 ± 0.005	−19.07 ± 3.08	84.94	88.06	0.4399	−18.93
NanE3	2.5	20	3	10	30	138.63 ± 9.34	88.57 ± 2.17	0.509 ± 0.002	−12.96 ± 1.99	139.79	88.57	0.5103	−13.00
NanE4	7.5	20	3	10	30	89.7 ± 8.16	88.67 ± 2.46	0.396 ± 0.004	−15.27 ± 1.36	89.28	88.67	0.3946	−15.27
NanE5	5.0	10	9	10	30	70.54 ± 7.89	85.26 ± 1.09	0.252 ± 0.003	−13.28 ± 1.68	70.3	85.32	0.2516	−13.32
NanE6	7.5	10	9	10	30	25.24 ± 5.36	90.67 ± 2.18	0.342 ± 0.006	−17.95 ± 1.84	25.17	90.73	0.3432	−17.95
NanE7	2.5	20	9	10	30	184.63 ± 13.67	85.55 ± 3.01	0.377 ± 0.008	−11.84 ± 1.67	184.23	85.54	0.3761	−11.82
NanE8	7.5	20	9	10	30	114.74 ± 12.01	91.39 ± 2.08	0.329 ± 0.005	−16.89 ± 1.09	114.73	91.38	0.3218	−16.92
NanE9	2.5	10	3	50	30	138.49 ± 14.25	93.68 ± 2.33	0.372 ± 0.006	−15.76 ± 1.82	138.55	93.75	0.3741	−15.81
NanE10	7.5	10	3	50	30	122.14 ± 13.49	86.78 ± 1.68	0.387 ± 0.004	−19.59 ± 1.73	122.05	86.85	0.3872	−19.60
NanE11	2.5	20	3	50	30	143.21 ± 15.97	94.76 ± 1.49	0.508 ± 0.005	−14.1 ± 0.91	142.2	94.75	0.5063	−14.09
NanE12	7.5	20	3	50	30	101.01 ± 10.59	88.29 ± 1.71	0.376 ± 0.007	−18.32 ± 2.37	101.34	88.28	0.3736	−18.36
NanE13	5.0	10	9	50	30	94.02 ± 10.06	89.42 ± 2.48	0.325 ± 0.006	−9.32 ± 0.48	94.08	89.44	0.3231	−9.31
NanE14	7.5	10	9	50	30	58.91 ± 8.27	88.26 ± 1.97	0.398 ± 0.008	−15.88 ± 1.89	58.6	88.28	0.3977	−15.93
NanE15	2.5	20	9	50	30	182.66 ± 15.11	90.48 ± 1.89	0.478 ± 0.003	−10.4 ± 1.67	182.97	90.48	0.4793	−10.23
NanE16	7.5	20	9	50	30	122.96 ± 12.93	89.75 ± 2.11	0.407 ± 0.006	−17.35 ± 1.76	123.12	89.75	0.4081	−17.34
NanE17	2.5	10	3	10	50	90.93 ± 9.01	93.07 ± 1.88	0.342 ± 0.009	−13.01 ± 1.84	90.61	93.15	0.3397	−12.88
NanE18	7.5	10	3	10	50	116.54 ± 13.27	93.87 ± 2.05	0.394 ± 0.001	−19.01 ± 2.38	116.39	93.95	0.3913	−19.43
NanE19	2.5	20	3	10	50	77.67 ± 12.09	90.61 ± 1.79	0.445 ± 0.006	−9.54 ± 1.52	77.26	90.6	0.4461	−9.54
NanE20	7.5	20	3	10	50	78.69 ± 11.22	91.84 ± 1.76	0.357 ± 0.001	−16.71 ± 1.81	78.67	91.83	0.3519	−16.57
NanE21	2.5	10	9	10	50	92.06 ± 9.94	90.68 ± 2.67	0.189 ± 0.006	−11.7 ± 2.36	92.07	90.72	0.1875	−11.70
NanE22	7.5	10	9	10	50	98.91 ± 8049	97.22 ± 2.98	0.304 ± 0.005	−21.22 ± 2.59	98.86	97.26	0.3005	−21.09
NanE23	2.5	20	9	10	50	163.98 ± 15.02	88.21 ± 3.01	0.318 ± 0.009	−10.96 ± 1.81	163.95	88.21	0.3179	−11.00
NanE24	7.5	20	9	10	50	146.24 ± 13.96	95.18 ± 2.93	0.284 ± 0.003	−20.87 ± 3.01	146.37	95.18	0.2851	−20.87
NanE25	2.5	10	3	50	50	125.58 ± 12.08	92.18 ± 2.64	0.408 ± 0.006	−9.80 ± 0.44	125.58	92.22	0.4009	−9.82
NanE26	7.5	10	3	50	50	161.38 ± 12.66	86.41 ± 2.59	0.437 ± 0.005	−18.49 ± 1.69	161.01	86.45	0.4355	−18.37
NanE27	2.5	20	3	50	50	86.87 ± 8.73	90.49 ± 1.99	0.538 ± 0.001	−8.86 ± 0.73	87.18	90.48	0.5391	−8.91
NanE28	7.5	20	3	50	50	98.08 ± 9.64	85.15 ± 3.13	0.427 ± 0.007	−17.93 ± 1.78	98.25	85.14	0.4279	−17.94
NanE29	2.5	10	9	50	50	123.63 ± 11.28	88.53 ± 1.64	0.355 ± 0.004	−5.90 ± 1.01	123.37	88.54	0.356	−5.96
NanE30	5.0	10	5	25	38	53.90 ± 4.01	92.56 ± 1.06	0.218 ± 0.007	−11.60 ± 0.031	54.64	91.05	0.223	−11.62
NanE31	2.5	20	9	50	50	170.09 ± 16.28	86.84 ± 1.43	0.517 ± 0.006	−7.7 ± 0.48	170.2	86.84	0.5182	−7.69
NanE32	7.5	20	9	50	50	162.54 ± 14.69	87.24 ± 1.62	0.468 ± 0.005	−19.5 ± 2.01	162.28	87.25	0.4684	−19.55
Axial points													
NanE33	0.946	15	6	30	40	130.04 ± 14.08	89.78 ± 1.38	0.512 ± 0.003	−6.65 ± 0.31	129.88	89.8	0.5115	−6.70
NanE34	10.946	15	6	30	40	95.95 ± 13.88	89.85 ± 3.03	0.580 ± 0.008	−23.87 ± 1.61	95.81	89.87	0.5823	−23.85
NanE35	5	3.107	6	30	40	86.02 ± 10.43	90.38 ± 2.87	0.165 ± 0.005	−15.27 ± 0.39	85.65	90.48	0.1588	−15.22
NanE36	5	26.892	6	30	40	146.42 ± 9.72	89.23 ± 1.56	0.298 ± 0.006	−12.88 ± 1.71	146.49	89.19	0.2977	−12.92
NanE37	5	15	1.135	30	40	106.86 ± 11.54	90.18 ± 2.16	0.426 ± 0.004	−12.76 ± 0.67	106.65	90.22	0.4243	−12.69
NanE38	5	15	13.135	30	40	129.94 ± 13.08	89.26 ± 2.49	0.249 ± 0.006	−13.44 ± 0.83	129.89	89.26	0.251	−13.47
NanE39	5	15	6	17.5683	40	108.41 ± 9.34	90.2 ± 1.94	0.395 ± 0.007	−10.03 ± 0.99	109.33	90.23	0.3908	−10.01
NanE40	5	15	6	77.568	40	141.71 ± 12.18	88.3 ± 1.83	0.347 ± 0.005	−13.51 ± 0.86	141.85	88.3	0.3487	−13.51
NanE41	5	15	6	30	16.2158	105.16 ± 8.97	88.45 ± 1.96	0.534 ± 0.004	−19.21 ± 1.64	104.97	88.49	0.5348	−19.25
NanE42	5	15	6	30	63.784	127.27 ± 11.86	91.16 ± 1.67	0.521 ± 0.006	−16.86 ± 1.00	127.18	91.18	0.5231	−16.82
Centre points													
NanE43	5	15	6	30	40	116.22 ± 11.76	89.8 ± 1.63	0.429 ± 0.005	−9.2 ± 0.41	116.07	89.83	0.4249	−9.20
NanE44	5	15	6	30	40	116.22 ± 11.76	89.8 ± 1.63	0.429 ± 0.005	−9.2 ± 0.41	116.07	89.83	0.4249	−9.20
NanE45	5	15	6	30	40	116.22 ± 11.76	89.8 ± 1.63	0.429 ± 0.005	−9.2 ± 0.41	116.07	89.83	0.4249	−9.20
NanE46	5	15	6	30	40	116.22 ± 11.76	89.8 ± 1.63	0.429 ± 0.005	−9.2 ± 0.41	116.07	89.83	0.4249	−9.20
NanE47	5	15	6	30	40	116.22 ± 11.76	89.8 ± 1.63	0.429 ± 0.005	−9.2 ± 0.41	116.07	89.83	0.4249	−9.20
NanE48	5	15	6	30	40	116.22 ± 11.76	89.8 ± 1.63	0.429 ± 0.005	−9.2 ± 0.41	116.07	89.83	0.4249	−9.20
NanE49	5	15	6	30	40	116.22 ± 11.76	89.8 ± 1.63	0.429 ± 0.005	−9.2 ± 0.41	116.07	89.83	0.4249	−9.20
NanE50	5	15	6	30	40	116.22 ± 11.76	89.8 ± 1.63	0.429 ± 0.005	−9.2 ± 0.41	116.07	89.83	0.4249	−9.20

Release study

A release study was performed to examine the release (*in vitro*) of PLP from the dissolution apparatus for the PLP-NE and CS-coated PLP-NE. Both optimized nanoemulsions were kept inside the dialysis bag separately in several measurements with both sides clipped to prevent any form of leakage. The sampling

time point chosen to withdraw the test sample (5.0 mL) was replaced by the same amount of fresh phosphate buffer. The *in vitro* release of paliperidone was determined using the LC-MS/MS method described in this research. All the results of the *in vitro* release of paliperidone were determined, and all these results fitted the Korsmeyer–Peppas model, zero-order, Higuchi model, and first-order.[12]

Paliperidone nanoemulsions used for the nasal permeation

Fresh nasal tissues were delicately acquired from the slaughterhouse to be used in the nasal cavities of goats. The area was fixed, *i.e.*, 0.785 cm^2 for nasal-tissue-cells for the permeation study using the Logan permeation instrument. The receptor chamber was filled with up to 20 millilitres of phosphate buffer containing pH (7.4) and maintained the temperature (37 °C). After the pre-incubation period of 20 minutes for each trial, we introduced the optimized PLP-NE and CS-PLP-NE into the donor chamber. After the pre-incubation period of 20 minutes for every trial, we introduced the optimized PLP-NE and CS-PLP-NE into the donor chamber. At specified time intervals, we extracted 1 mL of the sample from the receptor chamber. Subsequently, each of these samples underwent filtration using a 0.22μ membrane filter to prepare them for PLP analysis. The permeation of the PLP was then assessed using nasal tissues using the LC-MS method, as described by Ahmad *et al.*[12]

Loading capacity (LC) determination and stability evaluation of nanoemulsion

A previously described method was adapted to determine the loading capacity (LC).[31] The LC was calculated using eqn (1). NE is not thermodynamically stable unlike kinetically stable microemulsion. Nevertheless, their stability is usually maintained *via* either coalescence or Ostwald ripening. Hence, the stability profile of an optimized nanoemulsion (opt-PLP-NE) should be checked. Opt-PLP-NE was observed for the stability study for six months at 25 ± 1 °C, *i.e.* at room temperature. The long-storage stability of Opt-PLP-NE was observed under sonication. There were two conditions: one under the sonication of opt-PLP-NE, *i.e.* opt-NanE30 and another under the same nanoformulation without sonication, *i.e.* opt-NanEW30. We compared the major parameter, *i.e.* globule size for stability testing. We examined any alteration in the globule size of NE at the time of storage study after finishing the intervals, *i.e.* 0, 1, 2, 3, 4, 5, and 6 months.[12,31]

$$\mathrm{LC} = \frac{\text{initial quantity of PLP} - \text{free quantity of PLP}}{\text{total quantity of lipid used}} \times 100$$

Animal study

We obtained ethical approval for the PK and PD studies from the Green Research Lab Ethical Committee under reference GL-2021-08-027. Rats weighing between 200 and 300 grams were utilized in this study, with three rats housed together in each cage. These animals were subjected to a natural light–dark cycle and provided an easy approach to food and water within an environment maintained at a temperature of 20–30 °C and humidity levels in the range of 50–55%. Standard laboratory environmental conditions were maintained for all the animals. The study was conducted during the wake-up period of the animals, corresponding to the light cycle, when they were in an alert and active state.

Developing and validating an LC-MS method for paliperidone

We utilized LC-MS to create a bioanalytical method in accordance with U.S. FDA guidelines for the analysis of paliperidone in both brain tissue and plasma.[32] The linearity curve was plotted at eight different determined concentrations with the help of the calculation of the peak area ratio and $1/x^2$ weighed linear square regression.[12] The quality samples were prepared at different concentrations (LOQQC, LQC, MQC, and HQC) for various signal-to-noise ratios, *i.e.*, 10 : 1 was used to analyse the PLP amount after their extraction. We employed 6-pre-spiked extracted samples to establish the mean area response, comparing them with post-extraction spiked samples devoid of PLP in different matrices. We selected 6-distinct prepared samples for each QC level, including one calibration curve sample obtained through the separation of diverse matrices, such as plasma and brain homogenate. These samples were utilized to assess the validation parameters for inter- and intraday precision and accuracy calculations.

Parameters for UPLC-MS/MS analysis

For the quantification of PLP, we employed a highly sensitive and high-resolution mass spectrometer, specifically the LCMS-8045 from Kyoto, Japan, equipped with an ESI ionization source and a triple quadrupole mass analyzer. We utilized a Waters ACQUITY Column C-18 (100.0 mm; 1.70 μm) in conjunction with a UHPLC system featuring a binary solvent manager and an autosampler. We implemented specific mass spectrometry conditions, including a 1 minute scan time, a 0.02 seconds inter-scan delay, a 0.10 μ scan step at a rate of 30 000 μ s^{-1}, and the use of argon gas as the collision gas. To quantify PLP, we employed a collision energy of −19.0 eV in positive ion mode, and the mass transition *m*/*z* 427.21/207.20 was utilized for PLP quantification (Fig. 6). The analysis of PLP levels was conducted using Lab Solution Software Version 5.93 from Kyoto, Japan.

Sample preparation for CC and QC

We individually prepared PLP stock and PLP-IS solutions in methanol with a concentration of 1 mg mL^{-1}. Additionally, we generated eight distinct aqueous dilutions of PLP for the calibration curve using a stock solution of PLP. These eight dilutions were spiked with 2% for each concentration in various blank matrices, such as plasma and brain homogenate obtained from the animals. We can describe simply that means 2% spiking as adding 20 mL of aqueous PLP to 980 mL of a different blank matrix. Similarly, we prepared eight different PLP drug concentrations at various times, ranging from 1.0 to 2000.00 ng mL^{-1}, to create a calibration curve for all matrices. The same method was employed to prepare all QC samples,

with concentrations of 1.01 ng mL^{-1} for LLOQC, 2.90 ng mL^{-1} for LQC, 850.0 ng mL^{-1} for MQC, and 1600.0 ng mL^{-1} for HQC. These spiked dilutions were freshly prepared, and a temperature of 2–4 °C was used for storage.

Extraction of the matrix samples for bioanalysis

Freshly prepared calibration curves (CCs) and quality control (QC) samples were generated using unknown brain homogenates or plasma samples, which were subsequently collected for analysis. Spiked plasma samples were removed from the deep freezer and allowed to thaw in a water bath at room temperature. After thawing, we vigorously vortexed the samples to ensure thorough mixing. Pre-labelled polypropylene tubes were used to dispense IS dilution mixture (50 mL), containing ~250.0 ng mL^{-1} of paliperidone D4, for all samples except for the blank samples, for which 50 mL of dilution solution was added to maintain consistency. We introduced the sample (250 mL) into the container and mixed it by vortexing. Subsequently, we added a formic acid solution (5% v/v, 500 μL) and vortexed it again. The samples underwent extraction using the solid-phase extraction technique by employing a Waters Oasis HLB SPE cartridge with a capacity (1 cm^3, 30 mg). The cartridge underwent conditioning using a SpeeddiskÒ pressure processor, with a sequence involving the use of methanol (1.0 mL) and Milli-Q water (1.0 mL) under continuous positive pressure. Subsequently, we loaded the prepared plasma samples, followed by rinsing them with 2.0 mL of ultra-pure water, applied in two separate 1.0 mL increments. The cartridge was subjected to drying under positive pressure, followed by elution using methanol (1.0 mL). The eluted solution was then evaporated to dryness at 50 °C using a stream of nitrogen. Subsequently, the dried residue was reconstituted with mobile phase (250 mL) and transferred into autosampler vials for analysis using the LC-MS/MS system. The samples were carefully collected in HPLC vials to facilitate LC-MS quantification.

Pharmacokinetic parameter examination for the optimized nanoformulation of paliperidone

To investigate the pharmacokinetics, we established several experimental groups: Group 1 received PLP-S *via* intranasal administration, Group 2 received PLP-S intravenously, Group 3 received PLP-NE intranasally, Group 4 received PLP-nanoemulsion intravenously, and Group 5 received CS-coated PLP-nanoemulsion intranasally. In each case, we administered a 15 mg kg^{-1} dose of paliperidone drug to individual animals. At each designated sampling time, three rats were selected for the assessment of PK parameters across all experimental groups. Blood samples were initially collected from each animal, followed by the euthanization of the animals to obtain brain tissue for homogenization. The extraction of all matrices followed the same protocol outlined in the Bioanalytical extraction section for PK evaluation. We obtained samples at predetermined time intervals (including predoses, 30 minutes, 1, 2.0, 4, 8.0, 12.0, and 24 hours). These samples underwent the specified treatment procedures and were subsequently subjected to analysis using our in-house bioanalytical method to assess parameters such as $t_{1/2}$, K_e, C_{max}, and AUC_{0-t}. A single group consisted of twenty-four animals (8 animals per subgroup, totaling 24). Across all six groups, there were 144 animals, and each group received the specified dosage, as previously described. We first collected blood from each group of rats at each sampling point. After blood sampling, each rat was sacrificed, and the brain was collected to prepare brain homogenates for pharmacokinetic analysis. Each homogenate sample was individually prepared and subsequently analyzed using the LC-MS/MS method as outlined by Ahmad and colleagues in their 2023 study.[12]

Behavioral study

We conducted a behavioral analysis to investigate the antischizophrenic effectiveness of PLP. This research serves as a crucial instrument for exploring the roles of neurotransmitters in the brain that impact animals. We conducted all behavioral assessments during the daytime, specifically from 8:30 a.m. to 3:30 p.m. In this study, distinct sets of rats were utilized in testing the behavioral experiments detailed below.

Treatment

Ketamine (30.0 mg kg^{-1} intraperitoneally) was injected into animals daily for up to 5-consecutive days. Five animals were accommodated in each cage.

Open field locomotion activity test

We categorized the animals into four distinct groups as follows: Group 1 (Control) received a saline solution, Group 2 was administered ketamine at a dosage of 30.0 mg kg^{-1}, Group 3 received ketamine (30.0 mg kg^{-1}) in combination with PLP-NE (15 mg kg^{-1}), and Group 4 was treated with ketamine (30.0 mg kg^{-1}) along with PLP-MNE (15 mg kg^{-1}). We utilized the open field test (OFT) to assess exploratory activity and anxiety-like behavior in the animals, following the methodology established by Prut and Belzung.[33] The OFT was conducted in a dark rectangular wooden arena measuring 70 × 70 × 3 5 cm. Key parameters, such as total traveled distance, time spent in the center zone, grooming behavior, and vertical activity, were recorded in 10 minutes video segments, as described by Coronel-Oliveros *et al.*[34] Grooming behavior transitions were evaluated in accordance with the sequence outlined by Dam'azio *et al.*[35] and the protocols established by Coronel-Oliveros *et al.*[34] and Al-Nema *et al.*[36]

Evaluation of social interaction

We divided the animals into four groups: Group 1: Vehicle (Saline: Control), Group 2: Ketamine (30.0 mg kg^{-1}), Group 3: Ketamine (30.0 mg kg^{-1}) + PLP-NE (15 mg kg^{-1}), and Group 4: Ketamine (30.0 mg kg^{-1}) + PLP-MNE (15 mg kg^{-1}). We subjected the animals to 6 h of social isolation before conducting tests within a new and unfamiliar open field enclosure on the experimental day. The animals underwent evaluation in an unfamiliar open-field setting, where pairs of animals from the same experimental group (housed separately) encountered each

other for a 15 minutes duration. Consequently, we examined social behavior in pairs rather than on an individual basis. We manually documented the duration of the initial interactions, the frequency of social encounters, and the total interaction time in accordance with established methodologies.[36–39] We assessed social behavior using the Social Interaction Test (SIT), which was administered within an Open Field Test (OFT) arena with dimensions of 70 × 70 × 35 cm. We employed a modified version of the protocol introduced by File and Hyde.[38] We utilized two conspecific animals, one from the control or ketamine group and another untreated animal, with body weights differing by less than 10 grams. These animals were not isolated before the test. The Social Interaction Test (SIT) was conducted under low-stress conditions, featuring low lighting (17 °lux), a quiet environment, and a familiar arena after a two-day habituation period. We then analyzed the behavior of the rats in each pair. Importantly, each pair of rats was used only once in accordance with established methods.[36,37,40]

Forced swimming test

We investigated depression-like behavior using a modified version of the forced swimming test (FST), following the methodology outlined by Slattery and Cryan.[39] The modified version of the test involved increasing the water depth up to 30 cm, preventing the animal from stabilizing on the bottom using its tail. This adjustment extended the activity time and allowed us to analyze behavior patterns in the forced swimming test (FST) through three variables: swimming, immobilization, and climbing. Previous pharmacological studies have linked swimming behavior to serotonergic activity and climbing behavior to noradrenergic activity. Consequently, these variables provide valuable insights into the neurotransmission mechanisms underlying the depressive-like effects of various treatments. To enhance immobility, a pretest lasting 10 minutes was conducted 24 hours prior to the FST. We recorded videos for 5 minutes. The most prevalent behavior was quantified as scores at 5 seconds intervals within each 300 seconds video segment, following the approach outlined by Ahmad *et al.*[12] and Coronel-Oliveros *et al.*[34]

Statistical analysis

Statistical analysis involves the presentation of all results as mean ± SEM (Standard Error of Mean). Unpaired observations are compared using Student's *t*-test, and differences between groups are assessed through ANOVA, with significance indicated by the *p*-value.

Result and discussion

Selection of excipients for the formulation of the optimized nanoemulsion

We assessed the solubility of paliperidone in different oils, as outlined in Table 1, during the excipient screening process for the final formulation. Ultimately, we chose oleic acid as the oil component due to its superior solubility. Table 1 illustrates that Tween-80, with an HLB value of 15.00, exhibited the highest solubility, followed by Labrasol. Tween-80 was chosen as the surfactant primarily due to its ability to decrease particle size, which is attributed to its molecular weight, in contrast to other polymeric surfactants, as reported by Ghosh *et al.*[29]

Estimating the zeta potential is a critical characterization parameter used to assess the overall surface charge and stability of the optimized paliperidone nanoemulsion. The zeta potential values for the optimized paliperidone nanoemulsion nanoformulation ranged from −11.60 ± 0.031 to −21.22 ± 2.59 mV, as shown in Table 3. The negative zeta potential values observed in each paliperidone nanoemulsion (PLP-NE) may be attributed to the presence of negatively charged fatty acid esters within the oleic acid, as suggested by Ahmad *et al.*[24] Furthermore, the selection of oil and co-surfactant for the stable nanoformulation was guided by the assessment of ZP. Among the formulations, ClNE1 exhibited the lowest zeta potential (ζ = −11.60 mV), as detailed in Table 3. This formulation was based on the use of the surfactants Tween-80, PEG-400, and Labrasol, and it was subsequently chosen as the final combination. The choice of oleic acid is justified due to its well-documented health advantages, such as its potential for addressing infections, reducing inflammation, supporting the immune system, managing obesity, addressing cardiovascular issues, and promoting skin repair, as indicated in previous reports.[41–44] In addition, it is worth noting that nanoemulsions involving oleic acid and Tween 80 are less susceptible to Ostwald ripening, a phenomenon mentioned in previous research.[45] This suggests that the combination of oleic acid and Tween 80 holds promise for enhancing intranasal drug delivery.

The use of a combination of Tween-80 and Labrasol as surfactants and co-surfactants resulted in the formation of a highly transparent nanoemulsion (NE). This combination has been previously employed in other studies, where the inclusion of a hydrophilic co-surfactant was found to yield transparent microemulsions. These microemulsions exhibited very low zeta potential values, as demonstrated by Mahmoud *et al.*[44] It is known that non-ionic surfactants tend to induce a minimal zeta potential on the surface charge, subsequently leading to a reduction in the particle size of the nanoemulsion, as also observed by Ahmad *et al.*[24]

Placebo nanoemulsion optimized using a pseudoternary phase diagram

Different S_{mix} ratios were visually illustrated using PTPD, specifically highlighting the nanoemulsion region for enhanced clarity, as depicted in Fig. 1. Graphical representations of different S_{mix} ratios were generated using PTPD. Specifically, the nanoemulsion region was highlighted for better comprehension, as illustrated in Fig. 1. The concentration of surfactant increased as the S_{mix} ratio ranged from 1 : 2 to 4 : 1, resulting in an expanding nanoemulsion region. Specifically, S_{mix} 1 : 2 exhibited the smallest nanoemulsion region, while S_{mix} 4 : 1 exhibited the largest. The expansion of the nanoemulsion region correlated with an increase in the HLB (Hydrophilic–Lipophilic Balance) scale value, which was 15 (Tween-80). A higher HLB value for the S_{mix} 4 : 1 ratio led to increased viscosity

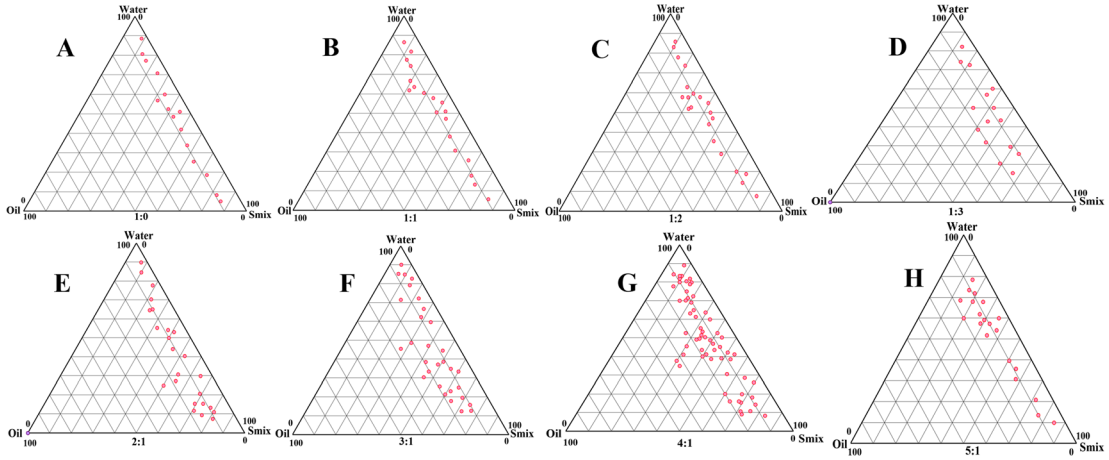

Fig. 1 Phase diagrams developed by applying the aqueous phase titration method for PLP-NE paliperidone zones (as dotted area) for oleic acid, Tween-80, Labrasol, and Milli-Q-water at S_{mix} ratios of 1 : 0 = (A), (B) = 1 : 1, (C) = 1 : 2, (D) = 1 : 3, (E) = 2 : 1, (F) = 3 : 1, (G) = 4 : 1 and (H) = 5 : 1.

in the nanoformulation, accompanied by the widest nanoemulsion region.[12] The PTPD was used to determine the smallest and greatest percentages of S_{mix} and oil.

Extensive evaluations were conducted on various combinations of oil, water, and S_{mix}, ultimately resulting in the selection of the top two combinations. Some of the combinations, particularly those with a greater oil percentage compared to the water percentage, were excluded due to the potential to form w/o emulsions. The lower limit for oil content was set at 5.0% to ensure the oil's effective drug-dissolving capacity, while the upper limit was capped at 10.0%. Beyond this concentration, the surfactant content exceeds 20%, promoting the formation of a microemulsion, as noted by Tadros *et al.*[16] This idea is consistent with the observation made by McClements[17] that a higher surfactant-to-oil ratio is necessary to create a microemulsion in contrast to a nanoemulsion, as also noted by Ahmed *et al.*[45]

Considering these corroborative data, the surfactant limits were chosen from 5.0 to 10.0%, reinforcing the optimization strategy. The preparation of Cur-NE was carried out using the ultrasonication technique, which was determined to be the most suitable method based on prior research findings.[24] The rationale for this approach is well founded in the fact that ultrasonication preserves the integrity of nanoemulsion globules. Five independent variables were selected for the optimization of the nanoemulsion formulation: oil content, S_{mix} ratio, ultrasonication time (minutes), ultrasonication intensity (%), and temperature (°C).

CCD software used to fit for optimized PLP-NE

The independent variables, such as the percentage of oil, percentage of S_{mix}, ultrasonication time (minutes), ultrasonication intensity (%), and temperature (°C), were chosen based on the findings from the previous studies mentioned above. Based on experimental values, we observed globule size, *i.e.*, (Y_1) (53.90–184.63 nm); % transmittance, *i.e.*, Y_2 (85.15–97.22%); Polydispersity Index (PDI), *i.e.*, Y_3 (0.165–0.580); and zeta potential (mV) *i.e.* Y_4 (from −6.65 to −23.87%). All the acquired data were input into the software for the optimization of the four dependent variables (DV) using polynomial quadratic optimization models ($p < 0.001$). Table 3 displays both the significant and non-significant variables, along with

Table 4 Results of regression analysis for responses Y_1 (particle size, nm), Y_2 (transmittance %), Y_3 (PDI), and Y_4 [zeta potential (mV)]

Quadratic model	R^2	Adjusted R^2	Predicted R^2	Standard deviation (SD)	% Coefficient of variation (CV)
Response (Y_1)	0.9995	0.9993	0.9992	0.8310	0.7185
Response (Y_2)	0.9938	0.9810	0.9925	0.2302	0.2562
Response (Y_3)	0.9909	0.9846	0.9871	0.0109	2.75
Response (Y_4)	0.9996	0.9994	0.9987	0.1071	0.7804

$Y_1 = +116.07 - 8.52 \times X_1 + 12.79 \times X_2 + 5.89 \times X_3 + 10.84 \times X_4 + 4.67 \times X_5 - 6.09 \times X_1X_2 - 4.75 \times X_1X_3 + 2.41 \times X_1X_4 + 12.98 \times X_1X_5 + 21.31 \times X_2X_3 - 6.26 \times X_2X_4 - 10.51 \times X_2X_5 - 0.9177 \times X_3X_4 + 10.56 \times X_3X_5 + 1.88 \times X_4X_5$ (eqn (1))

$Y_2 = +89.83 + 0.0172 \times X_1 - 0.2716 \times X_2 - 0.2416 \times X_3 - 0.6417 \times X_4 + 0.5654 \times X_5 + 0.1074 \times X_1X_2 + 1.44 \times X_1X_3 - 1.64 \times X_1X_4 + 0.2833 \times X_1X_5 + 0.0103 \times X_2X_3 + 0.2032 \times X_2X_4 - 0.6826 \times X_2X_5 - 0.3102 \times X_3X_4 + 0.1579 \times X_3X_5 - 1.57 \times X_4X_5$ (eqn (2))

$Y_3 = +0.4249 - 0.0049 \times X_1 + 0.0292 \times X_2 - 0.0294 \times X_3 + 0.0369 \times X_4 - 0.0025 \times X_5 - 0.0364 \times X_1X_2 + 0.0154 \times X_1X_3 - 0.0042 \times X_1X_4 + 0.0054 \times X_1X_5 + 0.0060 \times X_2X_3 + 0.0079 \times X_2X_4 + 0.0015 \times X_2X_5 + 0.0268 \times X_3X_4 + 0.0015 \times X_3X_5 + 0.0242 \times X_4X_5 + 0.0299 \times X_1^2 - 0.0348 \times X_2^2 - 0.0184 \times X_3^2 - 0.0290 \times X_4^2 + 0.0184 \times X_5^2$ (eqn (3))

$Y_4 = -9.20 - 3.41 \times X_1 + 0.4834 \times X_2 + 0.5511 \times X_3 + 0.6617 \times X_4 + 0.5116 \times X_5 - 0.1198 \times X_1X_2 - 0.7090 \times X_1X_3 - 0.5002 \times X_1X_4 - 1.19 \times X_1X_5 - 0.6590 \times X_2X_3 - 0.6065 \times X_2X_4 - 0.2016 \times X_2X_5 + 0.6704 \times X_3X_4 - 0.6608 \times X_3X_5 + 0.4317 \times X_4X_5 - 1.15 \times X_1^2 - 0.8610 \times X_2^2 - 0.9862 \times X_3^2 - 1.04 \times X_4^2 - 1.56 \times X_5^2$ (eqn (4))

adjustments made for all four DV using 'Adjustment of R^2'. The model fitting equations are shown in Table 4.

The individual interactive effects of X_1 (oil %), X_2 (S_{mix} %), X_3 (ultrasonication time in minutes), X_4 (ultrasonication intensity %), and X_5 (temperature in °C) are presented in eqn (1), as detailed in Table 4. For eqn (1), the percentage of oil showed a negative effect, but a positive effect was observed with all dependent variables Y_2, *i.e.*, transmittance (%); Y_3, *i.e.*, Polydispersity Index (PDI); and Y_4, *i.e.*, zeta potential (mV). On the contrary, a combination of independent variables exhibited a negative effect for % oil × % S_{mix} (X_1X_2), % S_{mix} × sonication time (X_1X_3), % S_{mix} × % ultrasonication intensity (X_2X_4), % S_{mix} × temperature °C (X_2X_5), and % ultrasonication intensity × temperature °C (X_3X_4), and positive effects was observed for % oil × % ultrasonication intensity (X_1X_4), % oil × temperature °C (X_1X_5), and % S_{mix} × ultrasonication time (X_2X_3), as shown in 5-dimensional plot for particle size in Fig. 2A.

We noticed that as the sonication time increased alongside the S_{mix} concentration, there was a subsequent reduction in the size of the NE globules. Through our observations, we noted an adverse impact on the reduction of NE globule size when the oil concentration was increased. Additionally, we observed that an enhancement in sonication time correlated positively with a higher percentage of transmittance and percentage of S_{mix}, which, in turn, increased the % oil content within the NE, as depicted in eqn (2) and Fig. 2B. Furthermore, we observed a favorable impact on % transmittance resulting from the combined influence of various factors, including the interactions between % oil × % S_{mix} (X_1X_2), % oil × ultrasonication time (X_1X_3), % oil × temperature °C (X_1X_5), % S_{mix} × ultrasonication time (X_2X_3), % S_{mix} × % ultrasonication intensity (X_2X_4), and ultrasonication time × temperature °C (X_3X_5).

The impact of independent variables on the polydispersity index is detailed in eqn (3), as illustrated in Fig. 2C. Our findings indicate that the polydispersity index increased with the enhancement of sonication intensity up to a certain threshold, but it exhibited a contrary response to the percentage of S_{mix} when compared to the increase in the concentration of oil. This observation contradicts the trends observed for percentage transmittance. Moreover, we observed a positive influence on the Polydispersity Index (PDI) due to the combined effects of various independent variables, including % oil × ultrasonication time (X_1X_3), % oil × % ultrasonication intensity (X_1X_4), % oil × temperature °C (X_1X_5), % S_{mix} × sonication time (X_2X_3), % S_{mix} × % ultrasonication intensity (X_2X_4), % S_{mix} × temperature °C (X_2X_5), ultrasonication time × % ultrasonication intensity (X_3X_4), ultrasonication time × temperature °C (X_3X_5), and % ultrasonication intensity × temperature °C (X_4X_5). Furthermore, certain adverse effects were observed, and they exhibited a negative magnitude, indicating a significant influence of ultrasonication time on the percentage of ultrasonication intensity, percentage of S_{mix}, and oil. This phenomenon could be attributed to the reduction in the size of NE globules, which, in turn, contributes to a smaller value of the polydispersity index. These effects were primarily associated with the variations in ultrasonication time and intensity.

The influence of independent variables on Zeta Potential (ZP) is depicted in eqn (4), as illustrated in Fig. 2D. Our findings indicate that ZP increased with a higher percentage of S_{mix} (v/v), longer duration of ultrasonication time (min), increased percentage of ultrasonication intensity, and higher °C of temperature. However, at a specific point, ZP showed a counter-response to the percentage of S_{mix} when compared to the increase in the strength of oil, which did not align with the trends observed for the percentage of transmittance.

We conducted the experiments under different conditions for the independent variables to identify an optimal formulation (Table 5). The independent variables, specifically the

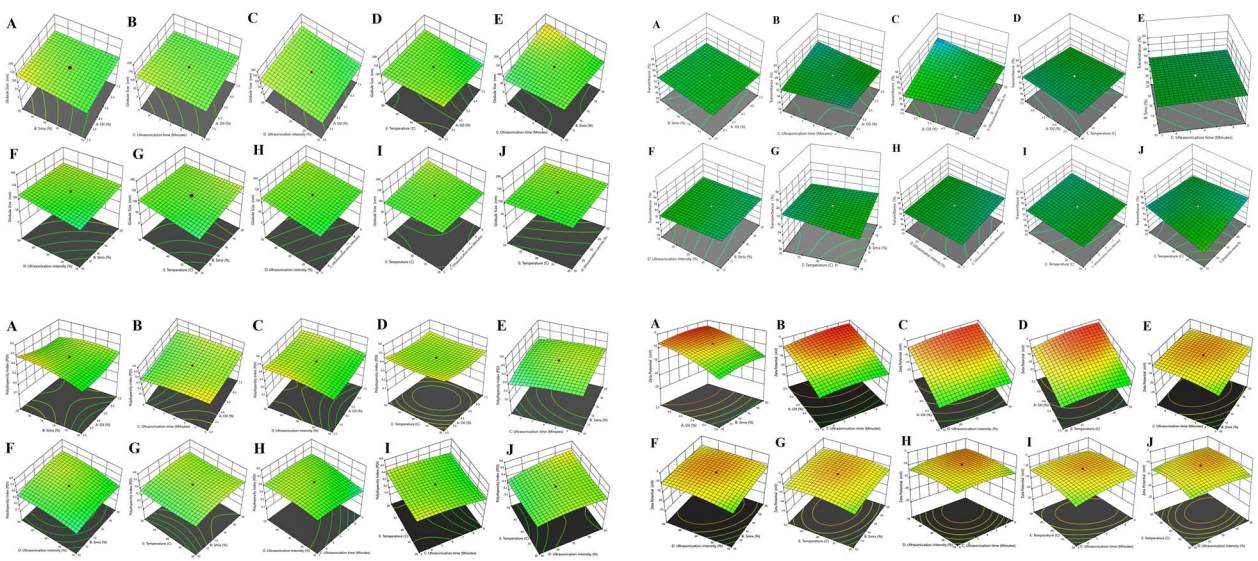

Fig. 2 (A) 3D response surface plots showing the interaction effect for Globule Size. (B) 3D response surface plots showing the interaction effect for percentage transmittance. (C) 3D response surface plots showing the interaction effect for the Polydispersity Index (PDI). (D) 3D response surface plots showing the interaction effect for zeta potential (mV).

Table 5 Best optimized and predicted batch of PLP-NE with independent variables, and dependent variables

	Independent variables					Dependent variables			
Batch	X_1	X_2	X_3	X_4	X_5	Y_1	Y_2	Y_3	Y_4
Predicted	5.0	9.997	4.987	24.968	37.698	54.64	91.05	0.223	−11.62
Optimized	5.0	10.0	5.00	25.00	38.00	53.90 ± 4.01	92.56 ± 1.06	0.218 ± 0.007	−11.60 ± 0.031

Some other characterized parameters of PLP-NE

PDI	Zeta potential (mV)	Refractive index	Viscosity (centipoise)	pH	Drug content (%)
0.218 ± 0.007	−11.60 ± 0.031	1.63 ± 0.029	35 ± 8 cp	7.4 ± 0.05	97.98 ± 0.39%

percentage of oil and ultrasonication time, were confined to a specified range, while the constraint for a percentage of S_{mix} was set to 'reduce'. Conversely, among the dependent variables, we aimed to 'reduce' both the value of globule size and polydispersity index and increase the value of the percentage of transmittance.

Based on the specified conditional parameters and the application of quadratic equations involving five independent variables, we optimized the formulation for PLP-NE using a Response Surface Methodology (RSM) with the following final composition: 5% of oil, 10% of S_{mix}, ultrasonication for 5 minutes, 25.0% of ultrasonication intensity, and a temperature of 38 °C. Subsequently, we predicted the properties of the optimized PLP-NE, which included a globule size of 53.90 ± 4.01 nm; percentage of transmittance, *i.e.*, 92.56 ± 1.06%; PDI of 0.218 ± 0.007; and a zeta potential of −11.60 ± 0.031, with an *R*-squared value of 0.9995.

Characterization of the PLP-nanoemulsion

A particle size of 53.90 nm was forecasted using the "CCD", and this closely matched the observed particle size of 53.90 ± 4.01 nm, as depicted in Fig. 3A. Additionally, the predicted PDI

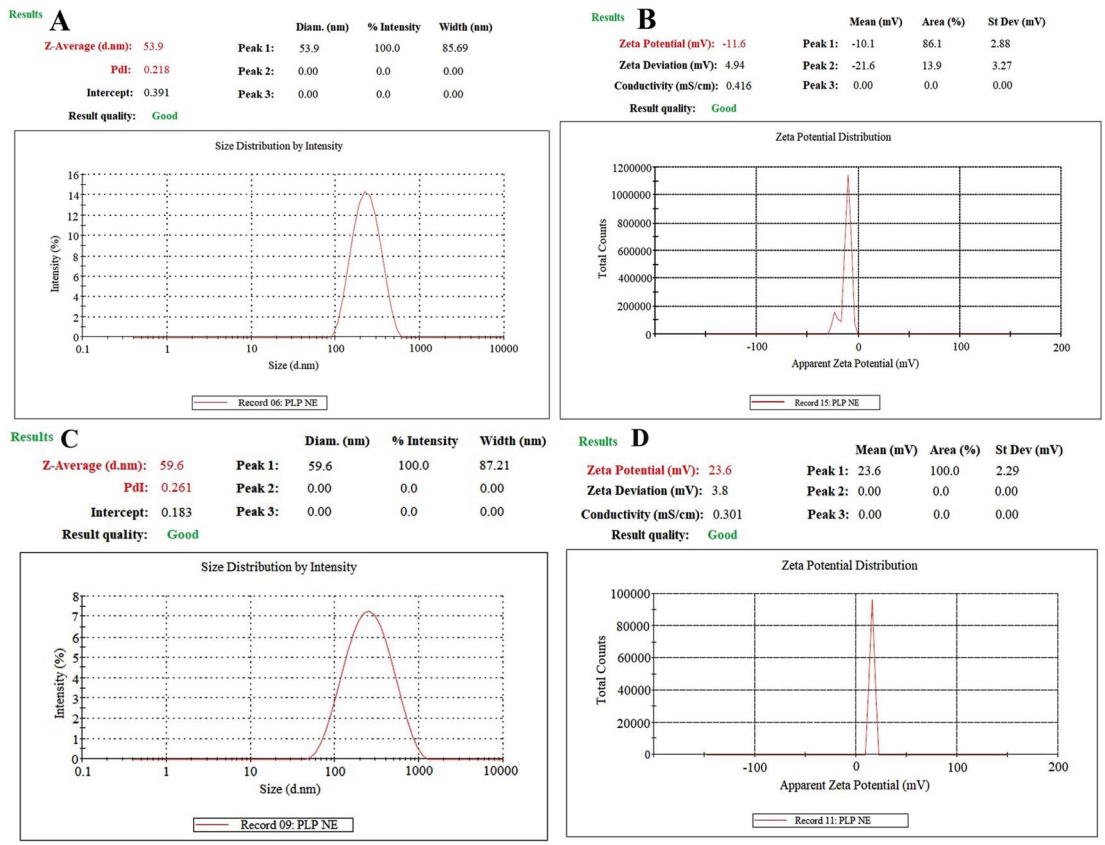

Fig. 3 Dynamic light scattering techniques for determining the particle size distribution of PLP-NE (A), zeta potential of PLP-NE (B), PLP-MNE (C), and zeta potential of PLP-MNE (D).

value (0.223) was in good agreement with the observed PDI value of 0.218 ± 0.007, indicating a size distribution of monomodal droplets, as shown in Fig. 3A. It was also "central composite design" software that provided a value for % transmittance (91.05), while the observed % transmittance was 92.56 ± 1.06% (Table 5).

Determination of zeta potential

The graph in Fig. 3B illustrates a ZP of −11.60 ± 0.031 mV for the optimized PLP-NE. This observation aligns with previous studies, such as the work conducted by Ghosh *et al.*,[29] which reported that non-ionic surfactant-stabilized oil droplets can exhibit a significant magnitude of droplet charge.

Characterization of mucoadhesive-optimized-PLP-NE

We used a 1% w/v chitosan solution to formulate a mucoadhesive-CS-PLP-NE formulation. The optimized mucoadhesive-CS-PLP-NE exhibited favorable characteristics, including a globule size of 59.60 ± 2.78 nm, a positive zeta potential (+23.60 ± 2.63 mV), and a very small polydispersity index of 0.261 ± 0.008 (see Fig. 3). Transmission Electron Microscopy (TEM) analysis confirmed globules with a size below 100 nm in CS-PLP-NE, displaying a spherical shape (as shown in Fig. 4), consistent with the results obtained from the Zetasizer. Furthermore, the CS-PLP-NE demonstrated a narrow globule size distribution, which was indicated by a low PDI value. Stability tests confirmed the thermodynamic stability of CS-PLP-NE, with a PDI consistently below 100 nm (Fig. 3). In terms of viscosity, PLP-NE displayed a viscosity of 35 ± 8 cp, while CS-PLP-NE exhibited a slightly higher viscosity at 42 ± 6 cp. These findings suggest that chitosan enhances the mucoadhesive properties of the optimized PLP-NE, aligning with our research objectives and prolonging the residence time in the treated area. This effect is attributed to the positive charge of chitosan interacting with the negatively charged mucosal surfaces, leading to a delayed and extended retention time, as discussed by Ahmad *et al.*[12]

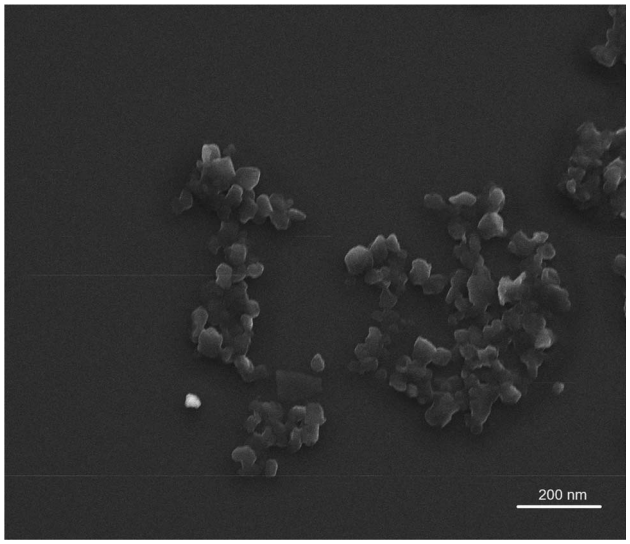

Fig. 4 Scanning electron microscopy (SEM) image of PLP-MNE.

SEM study

Scanning electron microscopy was used to characterize the morphology, dimensions, and surface texture of PLP-NE. The SEM images revealed a smooth and spherical surface for PLP-NE, as depicted in Fig. 4, with globule sizes measuring less than 100 nm, specifically 53.90 ± 4.01 nm.

Drug content and other parameter studies of PLP-NE characterization

The composition of PLP-NE was analyzed for viscosity, drug content, refractive index (RI), and pH. PLP-NE exhibited a very small dense and transparent formulation, characterized by an RI value of 1.62 ± 0.021. Additionally, it had a viscosity of 39 ± 6 cp and a pH of 7.40 ± 0.089. The drug content (PLP) in the optimized PLP-NE was found to be 97.98 ± 0.39% (see Table 5). The determination of drug content in the nanoemulsion involved dissolving 1 mL of the nanoformulation in methanol (10.0 mL). Subsequently, the mixture was subjected to shaking incubation (LSI-2005 RL, Lab Tech Co., Korea) at a speed of 50.00 rpm and a temperature of 37 ± 0.5 °C for half an hour, following the method described by Laxmi *et al.*[47] After this incubation period, the supernatant was taken and subjected to analysis using the LC-MS/MS method.

Release studies for optimized nanoemulsion of PLP and CS-based mucoadhesive-PLP-NE

Fig. 5A illustrates the release (*in vitro*) of PLP from both PLP-NE and mucoadhesive-optimized-CS-PLP-NE formulations. At the 24 hours mark, CS-PLP-NE exhibited a notably higher and controlled release, with a release percentage of 82.47 ± 6.01%, while PLP-NE showed a comparatively smaller release, with a percentage of 65.46 ± 5.45% for a total number of six (06) samples for each test. The enhanced release from CS-PLP-NE can be attributed to the nanosize of globules coated with chitosan, which provides a larger surface area for drug release, as discussed by Ahmad *et al.*[24] The release of PLP is paramount to achieving a rapid onset of action, characterized by an initial loading dose, followed by a controlled and extended release at the desired location. We assessed the release kinetics using various mathematical models, with the Higuchi matrix model exhibiting the highest correlation coefficient (R^2 = 0.9853). Following closely were the first order (R^2 = 0.9613), zero-order (R^2 = 0.9231), and Korsmeyer–Peppas models. The observed release profile holds significant value in achieving an early rapid drug release, which is crucial for establishing the required high concentration gradient necessary for successful intranasal drug delivery, as emphasized in a recent study by Ahmad *et al.*[12]

Intranasal permeation study of paliperidone from optimized nanoemulsion (*ex vivo*)

Permeation (*ex vivo*) studies of the nasal mucosa were conducted using both the PLP-NE and CS-PLP-NE formulations

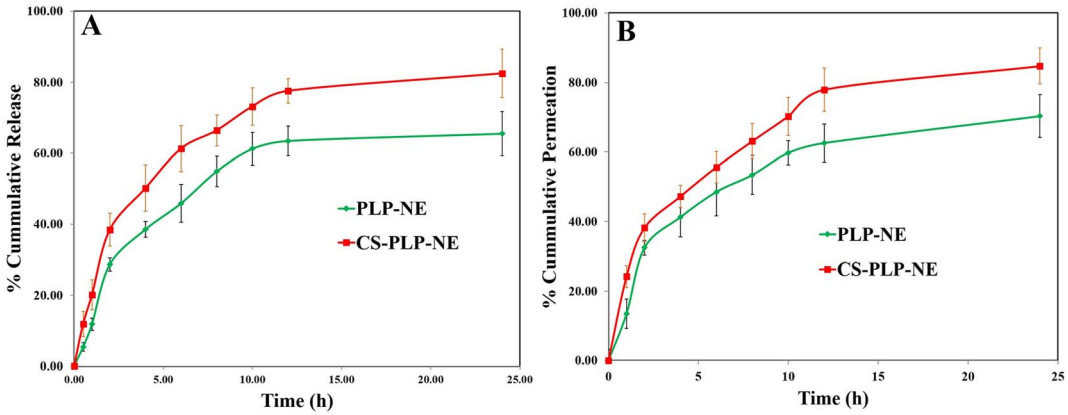

Fig. 5 Cumulative percentage release of paliperidone from PLP-MNE compared to PLP-NE: (A) *Ex vivo* permeation profiles of developed PLP-MNE compared to PLP-NE through goat nasal mucosa (B).

(Fig. 5B). Permeation studies were conducted on freshly collected goat nasal mucosa obtained from a local slaughterhouse. After 24 h, PLP-NE exhibited a permeation rate of 70.31 ± 6.19%, whereas CS-PLP-NE showed a higher permeation rate of 84.74 ± 5.14%. During the initial two hours, PLP-NE demonstrated a permeation rate of 32.45 ± 2.10%, which was lower compared to CS-PLP-NE, with a permeation rate of 38.14 ± 4.01%. PLP exhibited controlled delayed release *in vitro* while simultaneously demonstrating the highest *ex vivo* permeation through intranasal tissues. This behavior is attributed to the encapsulation of PLP within lipid globules within the NE, which is facilitated through both transcellular and paracellular pathways, as discussed by Ahmad *et al.*[12] CS-PLP-NE exhibited a higher steady-state flux, measuring at 5.93 ± 0.08 μg cm^{-2} h^{-1}, in contrast to PLP-NE, which recorded a lower flux of 3.79 ± 0.04 μg cm^{-2} h^{-1}. CS-PLP-NE demonstrated a higher permeability coefficient, measuring 5.64 × 10^{-3} ± 1.29 μg cm^{-2} h^{-1}, when compared to PLP-NE, which exhibited a lower coefficient of 2.68 × 10^{-3} ± 1.53 μg cm^{-2} h^{-1}. CS-mucoadhesive-PLP-NE displayed significantly improved permeation compared to PLP-NE, as evidenced by an enhancement ratio of 1.99. This enhancement can be attributed to the chitosan (CS) coating, as illustrated in Fig. 5B. The presence of mucoadhesive chitosan coating in PLP-NE extended the residence time on the nasal mucosa, allowing for prolonged and sustained drug action at the target site, as depicted in Fig. 5B.

Table 6 Total drug content of PLP-NE with storage at room temperature over the 6 months assessment period[a]

Time (months)	Drug loading (mg mL^{-1})	Drug recovery (mg mL^{-1})	Drug loss (%)
0	4.67 ± 3.45	4.60 ± 3.45	1.49
3	4.67 ± 3.45	4.52 ± 4.12	3.21
6	4.67 ± 3.45	4.46 ± 4.34	4.49

[a] Each value represents the mean ± standard deviation (n = 3). *Significant values relative to the initial drug loading at 0 months (Student's t-test, P < 0.05). Abbreviation: PLP-NE, paliperidone-loaded nanoemulsion.

Loading capacity (LC) determination and stability evaluation of nanoemulsion

As shown in Table 6, the actual loading capacity was 4.67 ± 3.45%, 1.49% of drug loss was observed at initial storage, and subsequent drug degradation was observed upon storage periods of 3 and 6 months with 3.21 and 4.49% of drug losses, respectively. Drug degradation was a challenging aspect of this study because it may affect the chemical and physical stabilities of the emulsion system. Opt-NanE30 formulated *via*

Table 7 PLP-NE showed stability results after their optimizations

	Optimized PLP-NE (sonication present) (opt-NanE30)			Optimized PLP-NE (no sonication) (opt-NanEW30)		
Duration (months)	Globule-size (nm) (n = 3)	PDI (n = 3)	Zeta potential (mV) (n = 3)	Globule-size (nm) (n = 3)	PDI (n = 3)	Zeta potential (mV) (n = 3)
0	53.90 ± 4.01	0.218 ± 0.007	−11.60 ± 0.031	73.63 ± 4.01	0.393 ± 0.007	−11.60 ± 0.031
1	54.09 ± 3.46	0.227 ± 0.008	−11.46 ± 0.028	99.96 ± 6.86	0.413 ± 0.006	−11.03 ± 0.022
2	62.93 ± 4.31	0.234 ± 0.006	−11.34 ± 0.029	169.32 ± 7.01	0.388 ± 0.005	−10.26 ± 0.038
3	71.34 ± 4.02	0.239 ± 0.008	−11.20 ± 0.033	197.61 ± 8.64	0.573 ± 0.009	−9.98 ± 0.041
4	86.79 ± 6.38	0.241 ± 0.007	−11.01 ± 0.027	236.18 ± 7.06	0.797 ± 0.007	−9.02 ± 0.037
5	100.31 ± 6.17	0.259 ± 0.006	−10.38 ± 0.026	329.26 ± 19.48	0.964 ± 0.008	−8.54 ± 0.052
6	108.72 ± 5.98	0.261 ± 0.007	−10.21 ± 0.037	Phase separation		

ultrasonication showed stability of up to fourteen weeks, but on the other side, opt-NanEW30 was manufactured without ultrasonication given the stability results of up to six months. The size of globule (53.90 ± 4.01), PDI (0.218 ± 0.007) and ZP (−11.60 ± 0.031) of opt-NanE30 was enhanced for up to zero to six months, as shown in Table 7, with great turbulence produced after ultrasonication as a greater rate of Ostwald ripening. At the time of Ostwald ripening, the globule size is enhanced by others, whereas the PDI of NE is enhanced, which means an unequal distribution of globule ions in terms of their size uniformity. The ZP of NE is enhanced, but it is an acceptable limit. We obtained the results for five to six months with an increase in globule size but not so much in the PDI and ZP, which confirms the stability of NE. We found that the results after twelve weeks suddenly increased the globule size. Moreover, for the size of the globule (73.63 ± 4.01), PDI (0.393 ± 0.007) and ZP (−11.60 ± 0.031) for opt-NanEW30, we initially obtained poor results because of the presence of micelles. We observed that the results after one month suddenly increased in the size of the globule (99.96 ± 6.86), PDI (0.413 ± 0.006), and ZP (−11.03 ± 0.022) for opt-NanEW30. However, we obtained a little bit of good PDI (0.413 ± 0.006) and ZP (−11.03 ± 0.022) for opt-NanEW30 (Table 7). The larger globule size is present at the time of ultrasonication in the NE, which is fractured or broken because of the collapse, production of the cavity, and preparation of the micro-jet, while the molecule of surfactant adsorbed the novel globules formed with a small size of globules, producing a uniform size NE.[12,31] Production of NE deprived of sonication that means-aqueous-micellar solution dissolves-oil & micelle swelling happens. We got the conclusion micelles which are participated in the preparation of NE gives the aggregation which results distract NE-stability.[12,31] ZP (−8.54 ± 0.052) is very small for the opt-NanEW30 illustrated stability for up to five months, which can be due to Tween-80 (non-ionic-surfactant), giving stability to NE.[12,31] From the stability study results, it was concluded that ultrasonic tailoring, followed by chemical engineering, might be helpful in increasing the stability of NE for a longer duration.

LC-MS results analysis

Fig. 6 and 7 display the MS and MS–MS scans for paliperidone (the analytes) and paliperidone-d4, respectively (used as the internal standard). Fig. 8 showcases all the chromatograms obtained for various samples: [A] brain homogenate (for blank), [B] blank extracted plasma, [C] extracted brain homogenate containing paliperidone (PLP), [D] plasma with extracted paliperidone (PLP), [E] extracted brain homogenate with paliperidone-d4, and [F] plasma with extracted paliperidone-d_4. Recovery, calculated from six replicates, yielded an average of greater than 81.49% for both brain homogenates and plasma. The developed method demonstrated linearity, with an *R*-squared (r^2) value exceeding 0.9995, within a concentration range of 1.0 to 2000.0 ng mL^{-1} for paliperidone (PLP). Selectivity for the developed method was established by analyzing chromatograms of blank plasma and brain homogenates (for blanks) to assess any interference with the detection of PLP. Table 8 provides a comprehensive dataset pertaining to the precision and accuracy of the optimized method, both inter-day and intra-day. The percentage precision for PLP across all quality control (QC) samples in brain homogenates and plasma fell within the range of 1.69–5.05% for both intra-batch and

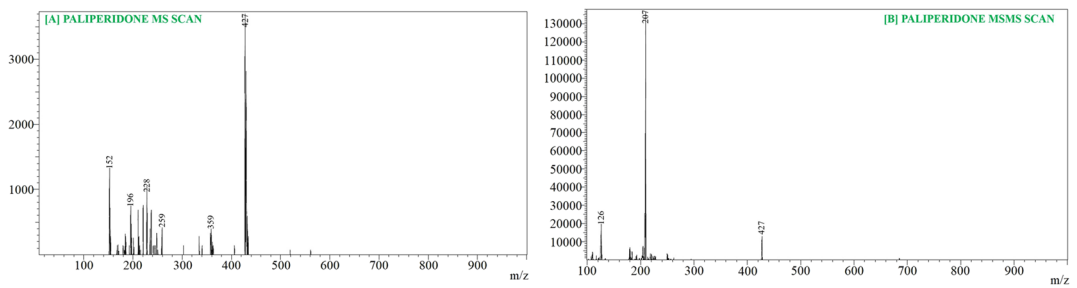

Fig. 6 Mass spectrum of (A) paliperidone (PLP) parent ion (protonated precursor $[M-H]^+$ ions at *m*/*z* 427.3) and (B) paliperidone (PLP) product ion (major fragmented product ion at *m*/*z* 207.15) showing fragmentation transitions.

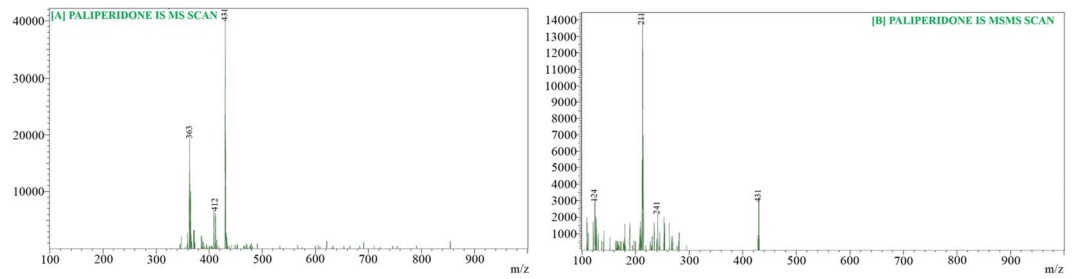

Fig. 7 Mass spectrum of (A) paliperidone-d4 (PLP-d4) parent ion (protonated precursor $[M-H]^+$ ions at *m*/*z* 431.2) and (B) paliperidone-d4 (PLP-d4) product ion (major fragmented product ion at *m*/*z* 211.2) showing fragmentation transitions.

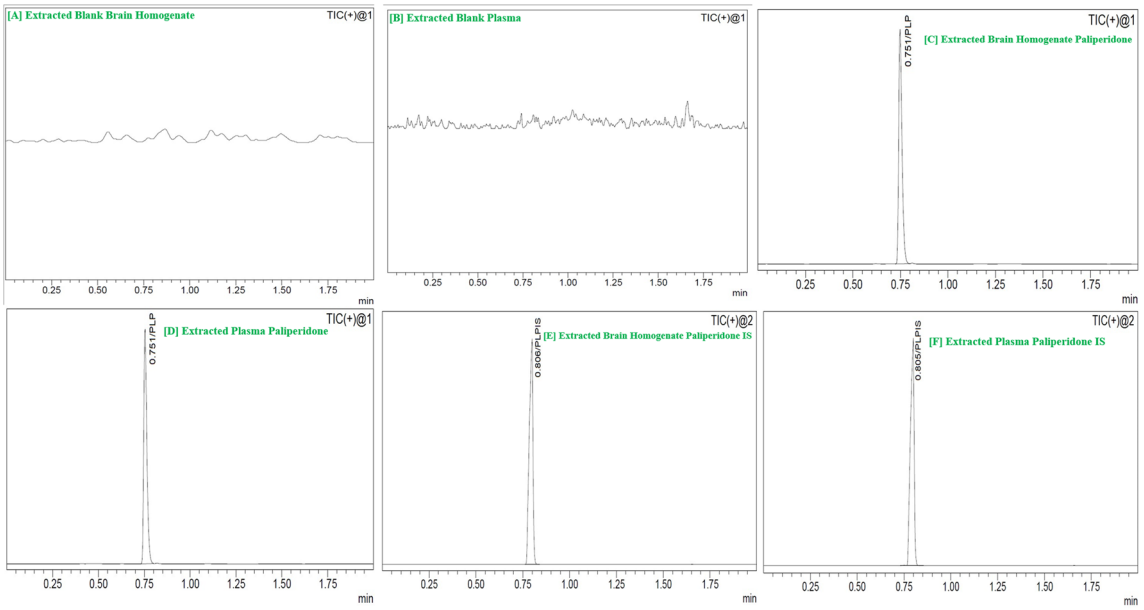

Fig. 8 Typical chromatograms of extracted blank plasma (A), extracted blank brain homogenate (B), extracted brain homogenate paliperidone (PLP) (C), plasma extracted paliperidone (PLP) (D), extracted brain homogenate paliperidone-IS (PLP-IS) (E), and plasma extracted paliperidone-IS (PLP-IS) (F).

inter-batch analyses. Similarly, the percentage accuracy for all QCs in both intra-batch and inter-batch assessments was observed in the range of 97.03% to 99.31% (Table 8). Furthermore, we conducted stability assessments for PLP, including freeze-thaw, long-term, post-processing, and benchtop stability. The results are shown in Table 9. The data indicate that PLP remained stable under these conditions, as discussed by Faiyazuddin *et al.*[46]

Pharmacokinetics analysis for the paliperidone study

The PK parameters were determined using the trapezoidal method, and a graph was created to illustrate the relationship between the PLP concentration in the brain and time. We utilized the trapezoidal method to ascertain the PK parameters; subsequently, a graph was generated to depict the relationship between the concentration of PLP in the brain and time. A single dose of PLP-S, PLP-NE, and CS-PLP-NE was administered through both intranasal and intravenous routes, as shown in Fig. 9. The maximum observed concentrations (C_{max}) of PLP-S were 81.28 ± 7.10 ng mL^{-1} (intravenous) and 116.14 ± 15.11 ng mL^{-1} (intranasal). Conversely, PLP-NE demonstrated C_{max} values of 138.62 ± 22.38 ng mL^{-1} (intravenous) and 991.35 ± 27.01 ng mL^{-1} (intranasal). Notably, CS-PLP-NE exhibited a significantly higher C_{max} of 163.49 ± 16.43 ng mL^{-1} (intravenous) and 1368.49 ± 45.18 ng mL^{-1} (intranasal), as indicated by the statistical significance levels: *p < 0.05, **p < 0.01, and ***p < 0.001, as shown in Table 10. Significantly elevated levels

Table 8 Validation: precision and accuracy data for Paliperidone (PLP) in different Biomatrixes

			Intra-batch precision			Inter-batch precision			
Biomatrix	Quality controls samples	Theoretical concentration (ng mL^{-1}) or (ng g^{-1})	Observed concentration (ng mL^{-1}) or (ng g^{-1}) ± S.D.	Accuracy[a] (%)	Precision[b] (% C.V.)	Observed concentration (ng mL^{-1}) or (ng g^{-1}) ± S.D.	Accuracy[a] (%)	Precision[b] (% C.V.)	Recovery[c] (%)
Brain homogenate	LOQQC	1.01	0.98 ± 0.04	97.03	4.08	0.99 ± 0.05	98.02	5.05	83.25
	LQC	2.90	2.88 ± 0.14	99.31	4.86	2.87 ± 0.13	98.97	4.53	81.64
	MQC	850.00	842.94 ± 17.41	99.17	2.07	840.31 ± 16.34	98.86	1.94	84.26
	HQC	1600.00	1580.31 ± 30.21	98.77	1.91	1575.61 ± 32.48	98.48	2.06	85.16
Plasma	LOQQC	1.01	0.99 ± 0.04	98.02	4.04	0.98 ± 0.03	97.03	3.06	82.14
	LQC	2.90	2.86 ± 0.13	98.62	4.55	2.85 ± 0.14	98.28	4.91	82.49
	MQC	850.00	840.36 ± 15.67	98.87	1.86	839.47 ± 16.21	98.76	1.93	86.24
	HQC	1600.00	1591.62 ± 28.41	99.06	1.78	1586.23 ± 26.86	99.14	1.69	81.49

[a] Values (mean ± SD) are derived from 6 replicates: Accuracy (%) = mean value of [(mean observed concentration)/(theoretical concentration)] × 100. [b] Precision (%): coefficient of variance (percentage) = standard deviation divided by mean concentration found × 100. [c] Recovery (%) = mean value of (peak height (mV) obtained from extracted biological sample)/(peak height (mV) obtained from the aqueous sample) × 100.

Table 9 Validation: stability data for Paliperidone (PLP) in different Biomatrixes[a]

	LQC (2.90 ng mL^{-1} or ng g^{-1})		MQC (850.0 ng mL^{-1} or ng g^{-1})		HQC (1600.0 ng mL^{-1} or ng g^{-1})	
Exposure condition	Brain homogenate	Plasma	Brain homogenate	Plasma	Brain homogenate	Plasma
Long term stability; recovery (ng) after storage (−80 °C)						
Previous day	2.88 ± 0.11	2.87 ± 0.11	843.69 ± 14.01	844.16 ± 13.64	1593.69 ± 18.36	1592.64 ± 13.61
30th day	2.81 ± 0.13 (97.57%)	2.80 ± 0.12 (97.56%)	833.21 ± 13.81 (98.76%)	828.14 ± 14.06 (98.10%)	1579.36 ± 16.66 (99.10%)	1578.24 ± 18.67 (98.10%)
Freeze–thaw stress; recovery (ng) after freeze–thaw cycles (−80 °C to 25 °C)						
Pre-cycle	2.89 ± 0.12	2.88 ± 0.09	845.36 ± 14.06	845.64 ± 7.83	1594.36 ± 16.68	1593.64 ± 17.48
First cycle	2.88 ± 0.13 (99.65%)	2.87 ± 0.11 (99.65%)	841.64 ± 13.11 (99.56%)	841.29 ± 9.16 (99.49%)	1581.36 ± 17.26 (99.18%)	1583.61 ± 18.94 (99.37%)
Second cycle	2.85 ± 0.12 (98.62%)	2.84 ± 0.12 (98.61%)	836.66 ± 14.28 (98.97)	839.09 ± 11.01 (99.23%)	1575.26 ± 16.35 (98.80%)	1571.64 ± 17.51 (98.62%)
Third cycle	2.83 ± 0.14 (97.92%)	2.81 ± 0.13 (97.57%)	829.11 ± 13.83 (98.08%)	837.15 ± 9.06 (99.00%)	1569.45 ± 17.98 (98.44)	1568.54 ± 25.21 (98.42%)
Bench top stability; recovery (ng) at room temperature (25 °C)						
0 h	2.88 ± 0.11	2.87 ± 0.09	846.09 ± 13.08	847.14 ± 6.99	1588.64 ± 12.54	1595.47 ± 16.47
24 h	2.84 ± 0.13 (98.61%)	2.82 ± 0.11 (98.26%)	836.94 ± 13.49 (98.92%)	829.66 ± 9.47 (97.94%)	1569.94 ± 18.21 (98.82%)	1577.42 ± 13.64 (98.87%)
Post processing stability; recovery (ng) after storage in auto sampler (4 °C)						
0 h	2.87 ± 0.12	2.88 ± 0.10	845.09 ± 9.66	846.14 ± 8.66	1589.64 ± 9.09	1594.36 ± 13.66
4 h	2.82 ± 0.14 (98.26%)	2.85 ± 0.11 (98.96%)	839.16 ± 8.34 (99.30%)	833.16 ± 9.03 (98.47%)	1585.29 ± 8.21 (99.73%)	1577.21 ± 11.24 (98.92%)

[a] Values (mean ± SD) are derived from six replicates. Figures in parentheses represent analyte concentration (%) relative to time zero. Theoretical contents: LQC: 2.90 ng mL^{-1}; MQC: 850.00 ng mL^{-1}; and HQC: 1600.00 ng mL^{-1}.

of intranasal AUC_{0-t} were noted, with values of 1147.02 ± 41.38 ng h mg^{-1} for PLP-S, 9593.03 ± 87.05 ng h mg^{-1} for PLP-NE, and 13 883.35 ± 143.27 ng h mg^{-1} for CS-PLP-NE. The statistical significance levels were denoted as *p < 0.05, **p < 0.01, and ***p < 0.001, respectively. CS-PLP-NE exhibits significantly higher values compared to PLP-S (intranasal) primarily due to the substantially improved C_{max} value and the extension of the elimination rate. Our research demonstrated enhanced brain bioavailability for all formulations (PLP-S, PLP-NE, and CS-PLP-NE) when administered intranasally, as opposed to other routes of administration. In conclusion, based on these findings, the intranasal route emerges as the optimal method for delivering PLP (the drug) to the brain, which aligns with previous research.[12]

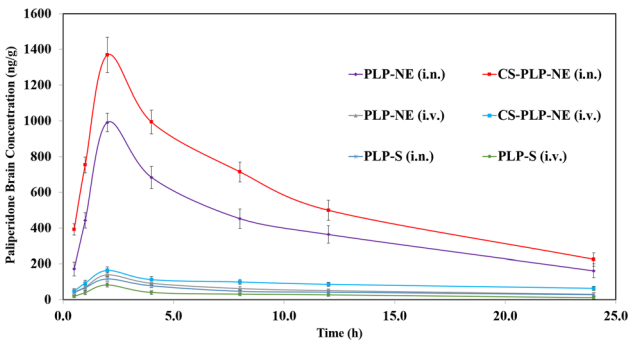

Fig. 9 Pharmacokinetic profiles of paliperidone concentration in the brain at various time intervals after administration of optimized CS-PLP-NE and optimized PLP-NE compared with PLP-S (pure).

Pharmacodynamic study (schizophrenia)

Open field locomotion activity test. Paliperidone's effects on ketamine-induced hyperlocomotion were assessed in a rat model. The rats were pre-treated with either a vehicle (*i.e.*, control group) or so many paliperidone formulations *via* different routes, 30 minutes prior to ketamine administration. Subsequently, their locomotion activity was assessed in a 5 minutes evaluation period following a 10 minutes acclimation period. Significance levels were denoted as $^{\#\#\#}P$ < 0.01 for the control group compared to the ketamine-treated model group, ***P < 0.01 for the Ketamine (25 mg kg^{-1}) + (CS-PLP-NE) intranasal group, **P < 0.01 for the Ketamine (25 mg kg^{-1}) + (PLP-NE) intranasal group, *P < 0.01 for the Ketamine (25 mg kg^{-1}) + (PLP-S) intranasal group, and *P < 0.01 for the Ketamine (25 mg kg^{-1}) + (PLP-S) oral group when compared to the ketamine-treated model group. The data are presented as the mean ± SD (n = 6) in Fig. 10.

Social interaction examination. The impact of paliperidone using a ketamine-induced model of social isolation was examined. Rats received ketamine injections for ten consecutive days, followed by a three-day undisturbed period. After a total of fourteen days, various paliperidone formulations were administered to different groups of rats *via* different routes, and their

Table 10 PK of paliperidone after i.n. and i.v. administration to rats at the dose of 15 mg kg $^{-1}$ in the brain, lungs and plasma ($n = 6$, mean ± SD)

Formulation administration	Samples	C_{max} (ng mL^{-1} g^{-1})	T_{max}	$t_{1/2}$ (h)	K_e (h^{-1})	AUC$_{0-t}$ (ng min mL^{-1} g^{-1})
PLP-S (i.n.)	Brain	116.14 ± 15.11	2.00	17.15 ± 3.21	0.04042 ± 0.0006	1147.02 ± 41.38
	Plasma	48.25 ± 3.16	0.50	7.63 ± 2.89	0.09083 ± 0.00075	172.89 ± 20.44
PLP-S (i.v.)	Brain	81.28 ± 7.10	2.00	12.98 ± 0.38	0.05339 ± 0.00079	664.57 ± 19.64
	Plasma	1566.39 ± 93.12	0.50	4.88 ± 0.71	0.14208 ± 0.00126	4440.75 ± 63.59
PLP-NE (i.n.)	Brain	991.35 ± 27.01	2.00	17.41 ± 4.03	0.03982 ± 0.00009	9593.03 ± 87.05
	Plasma	99.61 ± 4.01	2.00	10.95 ± 1.02	0.06331 ± 0.00010	679.71 ± 22.40
CS-PLP-NE (i.n.)	Brain	1368.49 ± 45.18	2.00	13.55 ± 6.38	0.05115 ± 0.00021	13 883.35 ± 143.27
	Plasma	139.16 ± 10.19	2.00	9.69 ± 0.99	0.07155 ± 0.00009	1058.88 ± 82.80
PLP-NE (i.v.)	Brain	138.62 ± 22.38	2.00	16.88 ± 3.18	0.04105 ± 0.00011	1357.39 ± 30.16
	Plasma	1029.46 ± 33.78	1.00	14.60 ± 1.96	0.04747 ± 0.00016	10 001.24 ± 173.04
CS-PLP-NE (i.v.)	Brain	163.49 ± 16.43	2.00	50.24 ± 5.34	0.01380 ± 0.00012	2110.46 ± 80.99
	Plasma	1466.29 ± 93.49	1.00	14.88 ± 1.15	0.04659 ± 0.00023	13 490.98 ± 282.94
PLP-S (i.n.)	Brain/plasma	2.41	4.00	2.25	0.45	6.63
PLP-S (i.v.)	Brain/plasma	0.05	4.00	2.66	0.38	0.15
PLP-NE (i.n.)	Brain/plasma	9.95	1.00	1.59	0.63	14.11
PLP-NE (i.v.)	Brain/plasma	0.13	2.00	1.16	0.86	0.14
CS-PLP-NE (i.n.)	Brain/plasma	9.83	1.00	1.40	0.71	13.11
CS-PLP-NE (i.v.)	Brain/plasma	0.11	2.00	3.38	0.30	0.16

Comparative bioavailability* (AUC$_{i.n.}$/AUC$_{i.v.}$); (%)

Formulations	PLP-S	PLP-NE	CS-PLP-NE
Blood	25.44	6.80	7.85
Brain	172.60***	706.73***	657.84***

social preferences were assessed. All rats underwent a 5 minutes evaluation following a 10 minutes acclimation period. Significance levels were represented as $^{###}P < 0.01$ for the control group compared to the ketamine-treated model group, $^{***}P < 0.01$ for the ketamine (25 mg kg^{-1}) + (CS-PLP-NE) intranasal group, $^{**}P < 0.01$ for the ketamine (25 mg kg^{-1}) + (PLP-NE) intranasal group, $^{*}P < 0.01$ for the ketamine (25 mg kg^{-1}) + (PLP-S) intranasal group, and $^{*}P < 0.01$ for the ketamine (25 mg kg^{-1}) + (PLP-S) oral group when compared to the ketamine-treated model group. Data are presented as the mean ± SD ($n = 6$) in Fig. 11.

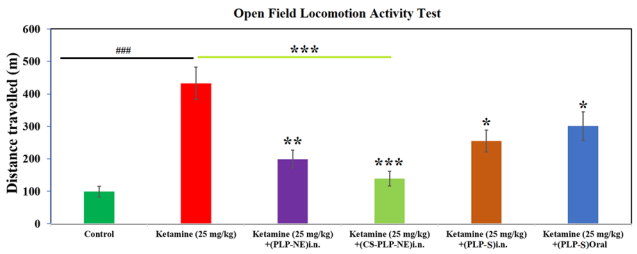

Fig. 10 Paliperidone effects on the ketamine-induced model hyperlocomotion in rats. Rats were pretreated with vehicle (control group) or various formulations of paliperidone of different groups with different routes 30 min before ketamine administration and then tested for locomotion activity. All rats were evaluated for 5 min after a 10 min period of acclimation. $^{###}P < 0.01$ value of control group compared to developed ketamine-treated model group, $^{***}P < 0.01$ value of ketamine (25 mg kg^{-1}) + (CS-PLP-NE)$_{i.n.}$ group, $^{**}P < 0.01$ value of ketamine (25 mg kg^{-1}) + (PLP-NE)$_{i.n.}$ group, $^{*}P < 0.01$ value of ketamine (25 mg kg^{-1}) + (PLP-S)$_{i.n.}$ group, and $^{*}P < 0.01$ value of Ketamine (25 mg kg^{-1}) + (PLP-S)$_{oral}$ group compared to developed ketamine-treated model group. Data are calculated as the mean ± SD ($n = 6$).

Forced swimming test results. The effects of paliperidone on a ketamine-induced model were assessed using the forced swimming test (FST) comparing different forms of preparations with control groups. Significance levels were represented as $^{###}P < 0.01$ for the control group compared to the ketamine-treated model group, $^{***}P < 0.01$ for the ketamine (25 mg kg^{-1}) + (CS-PLP-NE) intranasal group, $^{**}P < 0.01$ for the ketamine (25 mg kg^{-1}) + (PLP-NE) intranasal group, $^{*}P < 0.01$ for the ketamine (25 mg kg^{-1}) + (PLP-S) intranasal group, and $^{*}P < 0.01$ for the ketamine (25 mg kg^{-1}) + (PLP-S) oral group when compared to the ketamine-treated model group. Data are presented as the mean ± SD ($n = 6$) in Fig. 12.

Toxicological study of CS-PLP-NE

To assess the toxicological response of the optimized-CS-PLP-NE, we conducted a fourteen-day study, during which no instances of mortality were observed in any of the groups. Furthermore, no morphological changes were detected in terms of the microstructure of the brain or nasal mucosa tissues when compared to the control group (SHAM) following the administration of CS-NE (placebo), and CS-PLP-NE (treatment). Visual examination did not reveal any signs of inflammation or necrosis. These findings collectively indicate the safety profile of opt-CS-PLP-NE, as depicted in Fig. 13. In conclusion, the toxicity studies affirm the safety of the optimized CS-based mucoadhesive paliperidone nanoemulsion.[13]

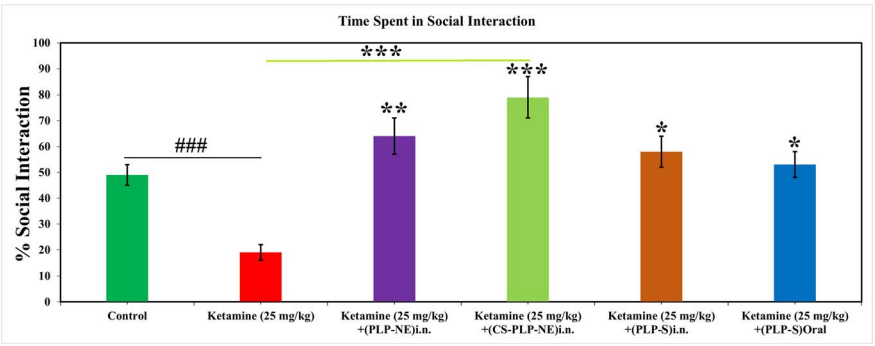

Fig. 11 Paliperidone effects on the ketamine-induced model of social isolation. Rats were injected with ketamine for 10 days and then left undisturbed for 3 days. Fourteen-day examination, vehicle (control group) and various formulations of paliperidone of different groups with different routes were injected, and rats were examined for social preferences. All rats were evaluated for 5 min after 10 min of acclimation. $^{###}P <$ 0.01 value of control group compared to developed ketamine-treated model group, $^{***}P < 0.01$ value of ketamine (25 mg kg^{-1}) + (CS-PLP-NE)$_{i.n.}$ group, $^{**}P < 0.01$ value of ketamine (25 mg kg^{-1}) + (PLP-NE)$_{i.n.}$ group, $^{*}P < 0.01$ value of ketamine (25 mg kg^{-1}) + (PLP-S)$_{i.n.}$ group, and $^{*}P < 0.01$ value of ketamine (25 mg kg^{-1}) + (PLP-S)$_{oral}$ group compared to the developed ketamine-treated model group. Data are calculated as the mean ± SD ($n = 6$).

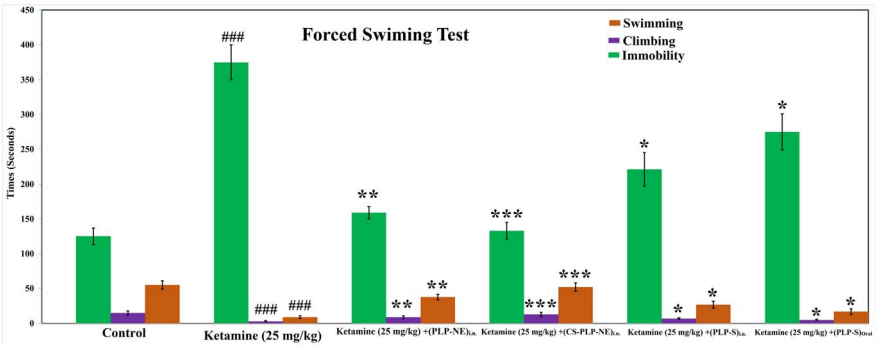

Fig. 12 Paliperidone effects on the ketamine-induced model as per examination of forced swimming test (FST) for different forms of preparations and their comparison with control groups. All rats were evaluated as per $^{###}P < 0.01$ value of the control group compared to the developed ketamine-treated model group, $^{***}P < 0.01$ value of ketamine (25 mg kg^{-1}) + (CS-PLP-NE)$_{i.n.}$ group, $^{**}P < 0.01$ value of ketamine (25 mg kg^{-1}) + (PLP-NE)$_{i.n.}$ group, $^{*}P < 0.01$ value of ketamine (25 mg kg^{-1}) + (PLP-S)$_{i.n.}$ group, and $^{*}P < 0.01$ value of ketamine (25 mg kg^{-1}) + (PLP-S)$_{oral}$ group compared to the developed ketamine-treated model group. Data are calculated as the mean ± SD ($n = 6$).

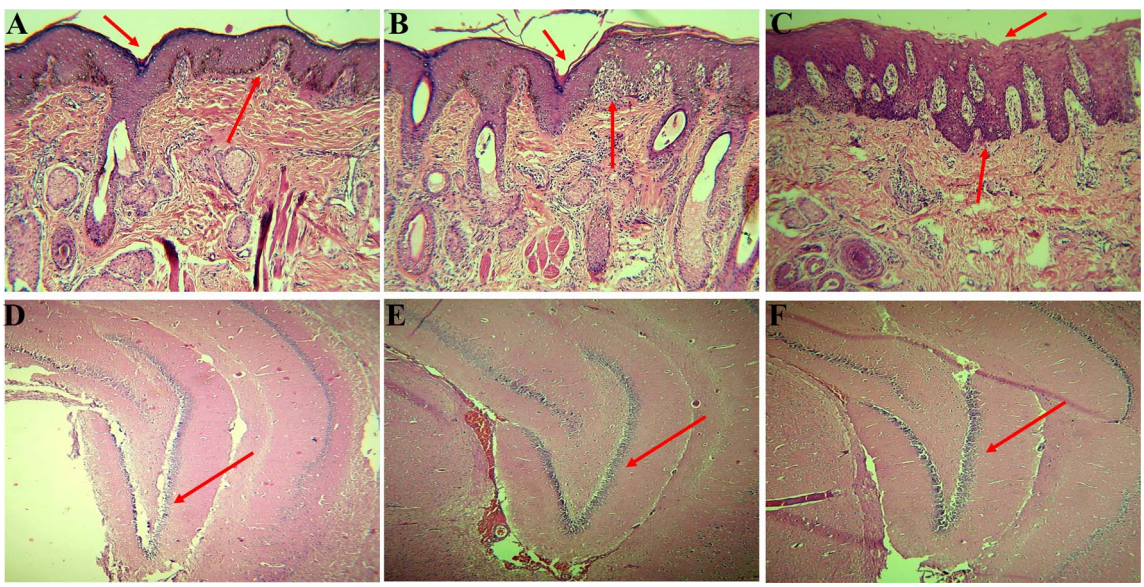

Fig. 13 Photomicrographs represent the transverse section of (A–C) images (Nasal Mucosa) and (D–F) images (Rat's brain) for the normal control, CS-NE (placebo), and CS PLP-NE-treated groups, respectively, after 14 days.

Conclusion

The nanoformulation of PLP-NE using the ultrasonication technique employs "Quality by Design" (QbD) software in the field of chemical engineering. After conducting pseudoternary phase examinations, it was determined that the S_{mix} ratio of 4 : 1 yielded the most extensive NE region among the various S_{mix} ratios tested. Chitosan was used as a mucoadhesive agent to develop the mucoadhesive-paliperidone nanoemulsion. CS-PLP-NE and PLP-NE showed a nanometre range (<100 nm) of globule size with smooth and round-shaped surface (as per SEM study), very small PDI, and best ZP in which PLP in higher amount. CS-PLP-NE showed a greater sustained release 24 h with higher permeability to the nasal mucosa, followed by maximum staying time in the nasal mucosa for the delivery of drug paliperidone into the brain to avoid the hepatic first pass-metabolism. A highly sensitive UHPLC-MS/Ms-based bio-analytical method was developed, validated and successfully applied for the determination of parameter biodistribution studies for CS-PLP-NE and PLP-NE. Paliperidone from CS-PLP-NE was found to be highly significant C_{max} and bioavailability of the brain compared to paliperidone nanoemulsion and PLP-S delivered through the i.n. route. We administered an extremely low dose of paliperidone using CS-PLP-NE *via* intranasal delivery for the treatment of schizophrenic rats based on highly significant results obtained from pharmacodynamic evaluations. These evaluations included assessments of Open field locomotion activity, social behaviour, swimming, climbing, and immobility parameters in the forced swimming tests, which were compared to the outcomes observed with PLP-NE and pure PLP-S. The optimized CS-based mucoadhesive paliperidone nanoemulsion is used in the treatment of schizophrenia by safely targeting the brain, with no toxic effects (based on rat's toxicity study results). A novel non-invasive industrial approach is poised to enter the market, pending further confirmation through clinical studies.

Data availability

The data that support the findings of this study are available on request.

Conflicts of interest

There is no conflict between the authors exists.

Acknowledgements

This study is supported *via* funding from "Prince Sattam Bin Abdulaziz University Project Number (PSAU/2024/R/1445)".

References

1 Y. Cao, F. Zhao, J. Chen, T. Huang, J. Zeng, L. Wang, X. Sun, Y. Miao, S. Wang and C. Chen, A simple and rapid LC-MS/MS method for the simultaneous determination of eight antipsychotics in human serum, and its application to therapeutic drug monitoring, *J. Chromatogr. B: Anal. Technol. Biomed. Life Sci.*, 2020, **1147**, 122129, DOI: 10.1016/j.jchromb.2020.122129.

2 S. Rehman, B. Nabi, A. Javed, T. Khan, A. Iqubal, M. J. Ansari, S. Baboota and J. Ali, Unraveling enhanced brain delivery of paliperidone-loaded lipid nanoconstructs: pharmacokinetic, behavioral, biochemical, and histological aspects, *Drug Delivery*, 2022, **29**(1), 1409–1422, DOI: 10.1080/10717544.2022.2069880.

3 G. Grunder, M. Heinze, J. Cordes, B. Mühlbauer, G. Juckel, C. Schulz, E. Rüther, J. Timm and N. S. Group, Effects of first-generation antipsychotics *versus* second-generation antipsychotics on quality of life in schizophrenia: a double-blind, randomised study, *Lancet Psychiatry*, 2016, **3**(8), 717–729, DOI: 10.1016/S2215-0366(16)00085-7.

4 C. M. Bellettato and M. Scarpa, Possible strategies to cross the blood–brain barrier, *Ital. J. Pediatr.*, 2018, **44**, 131, DOI: 10.1186/s13052-018-0563-0.

5 D. A. Sykes, H. Moore, L. Stott, N. Holliday, J. A. Javitch, J. R. Lane and S. J. Charlton, Extrapyramidal side effects of antipsychotics are linked to their association kinetics at dopamine D2 receptors, *Nat. Commun.*, 2017, **8**(1), 763, DOI: 10.1038/s41467-017-00716-z.

6 C. Dolder, M. Nelson and Z. Deyo, Paliperidone for schizophrenia, *Am. J. Health-Syst. Pharm.*, 2008, **65**, 403–413, DOI: 10.2146/ajhp070261.

7 G. Caruso, M. Grasso, A. Fidilio, G. Caruso, M. Grasso, A. Fidilio, F. Tascedda and F. Drago, Filippo Caraci, Antioxidant properties of second-generation antipsychotics: focus on microglia, *Pharmaceuticals*, 2020, **13**, 457, DOI: 10.3390/ph13120457.

8 K. Demirci, R. Ozcankaya, H. R. Yilmaz, A. Yiğit, A. C. Uğuz, K. Karakuş, A. Demirdaş and A. Akpınar, Paliperidone regulates intracellular redox system in rat brain: role of purine mechanism, *Redox Rep.*, 2015, **20**(4), 170–176, DOI: 10.1179/1351000214Y.0000000122.

9 K. S. MacDowell, J. R. Caso, D. Martın-Hernandez, J. L. Madrigal, J. C. Leza and B. García-Bueno, The atypical antipsychotic paliperidone regulates endogenous antioxidant or antiinflammatory pathways in rat models of acute and chronic restraint stress, *Neurotherapeutics*, 2016, **13**, 833–843, DOI: 10.1093/ijnp/pyu070.

10 B. Wilson, M. K. Samanta and K. Santhi, Poly(n-butylcyanoacrylate) nanoparticles coated with polysorbate80 for the targeted delivery of rivastigmine into the brain to treat Alzheimer's disease, *Brain Res.*, 2008, **1200**, 159–168, DOI: 10.1016/j.brainres.2008.01.039.

11 B. M. Shah, M. Misra, C. J. Shishoo and H. Padh, Nose to brain microemulsion-based drug delivery system of rivastigmine: formulation and ex-vivo characterization, *Drug Delivery*, 2015, **22**(7), 918–930, DOI: 10.3109/10717544.2013.878857.

12 N. Ahmad, M. S. Khalid, A. M. Al Ramadhan, M. Z. Alaradi, M. R. Al Hammad, K. Ansari, Y. D. Alqurashi, M. F. Khan, A. A. Albassam, M. J. Ansari, S. Akhtar and M. Dilshad, Preparation of melatonin novel-mucoadhesive nanoemulsion used in the treatment of depression, *Polym.*

Bull., 2023, **80**, 8093–8132, DOI: 10.1007/s00289-022-04436-3.

13 N. Ahmad, M. J. A. Al-Ghamdi, H. S. M. Alnajjad, B. B. A. Al Omar, M. F. Khan, Z. S. Al malki, A. A. Al Bassam, Z. Ullah, M. S. Khalid and K. Ashraf, A comparative brain Toxico-Pharmacokinetics study of a developed tannic acid nanoparticles in the treatment of epilepsy, *J. Drug Delivery Sci. Technol.*, 2022, **76**, 103772, DOI: 10.1016/j.jddst.2022.103772.

14 N. Ahmad, S. Umar, M. Ashafaq, M. Akhtar, Z. Iqbal, M. Samim and F. J. Ahmad, A comparative study of PNIPAM nanoparticles of curcumin, demethoxycurcumin, and bisdemethoxycurcumin and their effects on oxidative stress markers in experimental stroke, *Protoplasma*, 2013, **250**, 1327–1338, DOI: 10.1007/s00709-013-0516-9.

15 C. Qian and D. J. McClements, Formation of nanoemulsions stabilized by model food-grade emulsifiers using high-pressure homogenization: Factors affecting particle size, *Food Hydrocolloids*, 2011, **25**(5), 1000–1008, DOI: 10.1016/j.ultsonch.2017.09.042.

16 T. Tadros, P. Izquierdo, J. Esquena and C. Solans, Formation and stability of nanoemulsions, *Adv. Colloid Interface Sci.*, 2004, **108–109**, 303–318, DOI: 10.1016/j.cis.2003.10.023.

17 D. J. McClements, Nanoemulsions *versus* microemulsions: terminology, differences, and similarities, *Soft Matter*, 2012, **8**, 1719–1729, DOI: 10.1039/C2SM06903B.

18 M. Sivakumar, S. Y. Tang and K. W. Tan, Cavitation technology – A greener processing technique for the generation of pharmaceutical nanoemulsions, *Ultrason. Sonochem.*, 2014, **21**, 2069–2083, DOI: 10.1016/j.ultsonch.2014.03.025.

19 M. L. A. Baig and S. A. Ali, LC-MS/MS Method for the Estimation of Paliperidone in Human Plasma, *Anal. Chem. Lett.*, 2017, **7**(2), 228–240, DOI: 10.1080/22297928.2017.1333039.

20 S. A. Jadhav, S. B. Landge, P. M. Choudhari, P. V. Solanki, S. R. Bembalkar and V. T. Mathad, Stress Degradation Behavior of Paliperidone, an Antipsychotic Drug, and Development of Suitable Stability-Indicating RP-LC Method, *Chromatogr. Res. Int.*, 2011, **2011**(256812), 1–12, DOI: 10.4061/2011/256812.

21 M. Z. Bocato, R. A. Simões, L. A. Calixto, C. M. de Gaitani, M. T. Pupo and A. R. M. de Oliveira, Solid phase microextraction and LC-MS/MS for the determination of paliperidone after stereoselective fungal biotransformation of risperidone, *Anal. Chim. Acta*, 2012, **742**, 80–89, DOI: 10.1016/j.aca.2012.05.056.

22 J. Sim, E. Kim, W. Yang, S. Woo and S. In, An LC-MS/MS method for the simultaneous determination of 15 antipsychotics and two metabolites in hair and its application to rat hair, *Forensic Sci. Int.*, 2017, **274**, 91–98, DOI: 10.1016/j.forsciint.2017.01.001.

23 C. Ruggiero, S. Ramirez, E. Ramazzotti, R. Mancini, R. Muratori, M. A. Raggi and M. Conti, Multiplexed therapeutic drug monitoring of antipsychotics in dried plasma spots by LC-MS/MS, *J. Sep. Sci.*, 2020, **43**(8), 1440–1449, DOI: 10.1002/jssc.201901200.

24 N. Ahmad, R. Ahmad, A. Al-Qudaihi, S. E. Alaseel, I. Z. Fita, M. S. Khalid and F. H. Pottoo, Preparation of a novel curcumin nanoemulsion by ultrasonication and its comparative effects in wound healing and the treatment of inflammation, *RSC Adv.*, 2019, **9**, 20192–20206, DOI: 10.1039/C9RA03102B.

25 Y. Sangsen, K. Wiwattanawongsa, K. Likhitwitayawuid, B. Sritularak, P. Graidist and R. Wiwattanapatapee, Influence of surfactants in self-microemulsifying formulations on enhancing oral bioavailability of oxyresveratrol: studies in Caco-2 cells and in vivo, *Int. J. Pharm.*, 2016, **498**(1–2), 294–303, DOI: 10.1016/j.ijpharm.2015.12.002.

26 Po-H. Li and B.-H. Chiang, Process optimization and stability of D-limonenein-water nanoemulsions prepared by ultrasonic emulsification using response surface methodology, *Ultrason. Sonochem.*, 2012, **19**(1), 192–197.

27 S. K. Singh, P. Dadhania, P. R. Vuddanda, A. Jain, S. Velaga and S. Singh, Intranasal delivery of asenapine loaded nanostructured lipid carriers: formulation, characterization, pharmacokinetic and behavioural assessment, *RSC Adv.*, 2016, **6**, 2032–2045.

28 T. Delmas, H. Piraux, A. C. Couffin, I. Texier, F. Vinet, P. Poulin, M. E. Cates and J. Bibette, How to prepare and stabilize very small nanoemulsions, *Langmuir*, 2011, **27**(5), 1683–1692.

29 V. Ghosh, A. Mukherjee and N. Chandrasekaran, Ultrasonic emulsification of food-grade nanoemulsion formulation and evaluation of its bactericidal activity, *Ultrason. Sonochem.*, 2013, **20**(1), 338–344.

30 N. C. Loong, M. Basri, L. F. Fang, H. R. F. Masoumi, M. Tripathy, R. A. Karjiban and E. Abdul-Malek, Comparison of Box-Behnken and central composite designs in optimization of fullerene loaded palm-based nano-emulsions for cosmeceutical application, *Ind. Crops Prod.*, 2014, **59**, 309–317.

31 S. Özdemir, B. Çelik, E. T. Acar, G. Duman and M. Üner, Eplerenone Nanoemulsions for Treatment of Hypertension. Part I: Experimental Design for Optimization of Formulations and Physical Characterization, *J. Drug Delivery Sci. Technol.*, 2018, **45**, 357–366, DOI: 10.1016/j.jddst.2018.03.011.

32 US FDA, Guidance for Industry Bioanalytical Method Validation, 2001, available from: http://www.fda.gov/downloads/Drugs/GuidanceComplianceRegulatoryInformation/Guidances/UCM070107.pdf, last accessed on 2018 May 24.

33 L. Prut and C. Belzung, The open field as a paradigm to measure the effects of drugs on anxiety-like behaviors: A review, *Eur. J. Pharmacol.*, 2003, **463**(1), 3–33.

34 C. M. Coronel-Oliveros and R. Pacheco-Calderón, Prenatal exposure to ketamine in rats: Implications on animal models of schizophrenia, *Dev. Psychobiol.*, 2018, **60**(1), 30–42, DOI: 10.1002/dev.21586.

35 F. Damazio Pacheco, L. Canever, G. Mastella, P. G. Wessler, A. K. Godoi, I. Hubbe, A. da Costa Afonso, D. Celso, J. Quevedo and A. I. Zugno, Effects of ketamine on

prepubertal Wistar rats: Implications on behavioral parameters for Childhood-Onset Schizophrenia, *Int. J. Dev. Neurosci.*, 2019, **79**, 49–53, DOI: 10.1016/j.ijdevneu.2019.10.006.

36 M. Al-Nema, A. Gaurav, M. T. Lee, P. Okechukwu, P. Nimmanpipug and V. S. Lee, Evaluation of the acute oral toxicity and antipsychotic activity of a dual inhibitor of PDE1B and PDE10A in rat model of schizophrenia, *PLoS One*, 2022, **17**(12), e0278216, DOI: 10.1371/journal.pone.0278216.

37 R. J. Niesink and J. M. V. Ree, Involvement of opioid and dopaminergic systems in isolation-induced pinning and social grooming of young rats, *Neuropharmacology*, 1989, **28**(4), 411–418, DOI: 10.1016/0028-3908(89)90038-5.

38 S. E. File and J. R. G. Hyde, Can social interaction be used to measure anxiety?, *Br. J. Pharmacol.*, 1978, **62**(1), 19–24.

39 D. A. Slattery and J. F. Cryan, Using the rat forced swim test to assess antidepressant-like activity in rodents, *Nat. Protoc.*, 2012, **7**(6), 1009–1014, DOI: 10.1038/nprot.2012.044.

40 L. Canever, L. Oliveira, R. D. de Luca, P. T. Correa, D. B. Fraga, M. P. Matos, G. Scaini, J. Quevedo, E. L. Streck and A. I. Zugno, A rodent model of schizophrenia reveals increase in creatine kinase activity with associated behavior changes, *Oxid. Med. Cell. Longevity*, 2010, **3**(6), 421–427, DOI: 10.4161/oxim.3.6.13446.

41 H. Sales-Campos, P. R. de Souza, B. C. Peghini, J. S. da Silva and C. R. Cardoso, An overview of the modulatory effects of oleic acid in health and disease, *Mini-Rev. Med. Chem.*, 2013, **13**(2), 201–210, DOI: 10.2174/1389557511313020003.

42 H. Tutunchi, A. Ostadrahimi and M. Saghafi-Asl, The Effects of Diets Enriched in Monounsaturated Oleic Acid on the Management and Prevention of Obesity: a Systematic Review of Human Intervention Studies, *Adv. Nutr.*, 2020, **11**(4), 864–877, DOI: 10.1093/advances/nmaa013.

43 A. S. Hadi and M. M. Ghareeb, Rizatriptan Benzoate Nanoemulsion for Intranasal Drug Delivery: Preparation and Characterization, *Int. J. Drug Deliv. Technol.*, 2022, **12**(2), 546–552, DOI: 10.25258/ijddt.12.2.14.

44 D. B. Mahmoud, M. M. Bakr, A. A. Al-Karmalawy, Y. Moatasim, A. El Taweel and A. Mostafa, Scrutinizing the Feasibility of Nonionic Surfactants to Form Isotropic Bicelles of Curcumin: a Potential Antiviral Candidate Against COVID-19, *AAPS PharmSciTech*, 2021, **23**(1), 44, DOI: 10.1208/s12249-021-02197-2.

45 S. Ahmed, A. Gull, M. Alam, M. Aqil and Y. Sultana, Ultrasonically tailored, chemically engineered and "QbD" enabled fabrication of agomelatine nanoemulsion; optimization, characterization, ex vivo permeation and stability study, *Ultrason. Sonochem.*, 2018, **41**, 213–226, DOI: 10.1016/j.ultsonch.2017.09.042.

46 M. Faiyazuddin, N. Ahmad, R. K. Khar, A. Bhatnagar and F. J. Ahmad, Stabilized terbutaline submicron drug aerosol for deep lungs deposition: drug assay, pulmonokinetics and biodistribution by UHPLC/ESI-q-TOF-MS method, *Int. J. Pharm.*, 2012, **434**(1–2), 59–69, DOI: 10.1016/j.ijpharm.2012.05.007.

47 M. Laxmi, A. Bhardwaj, S. Mehta and A. Mehta, Development and characterization of nanoemulsion as carrier for the enhancement of bioavailability of artemether, *Artif. Cells, Nanomed., Biotechnol.*, 2015, **43**(5), 334–344, DOI: 10.3109/21691401.2014.887018.